

# Metrics Revolutions: Groundbreaking Insights into the Implementation of Metrics for Biomedical Image Segmentation

Gašper Podobnik and Tomaž Vrtovec

University of Ljubljana, Faculty of Electrical Engineering, Tržaška cesta 25, SI-1000 Ljubljana, Slovenia.

## Abstract

The evaluation of segmentation performance is a common task in biomedical image analysis, with its importance emphasized in the recently released metrics selection guidelines and computing frameworks. To quantitatively evaluate the alignment of two segmentations, researchers commonly resort to counting metrics, such as the Dice similarity coefficient, or distance-based metrics, such as the Hausdorff distance, which are usually computed by publicly available open-source tools with an inherent assumption that these tools provide consistent results. In this study we questioned this assumption, and performed a systematic implementation analysis along with quantitative experiments on real-world clinical data to compare 11 open-source tools for distance-based metrics computation against our highly accurate mesh-based reference implementation. The results revealed that statistically significant differences among all open-source tools are both surprising and concerning, since they question the validity of existing studies. Besides identifying the main sources of variation, we also provide recommendations for distance-based metrics computation.

**Keywords:** Biomedical image analysis, Medical imaging, Validation metrics, Objective evaluation, Semantic segmentation, Instance segmentation, Benchmarking, Method comparison, Hausdorff distance, Percentile of Hausdorff distance, Mean average surface distance, Average symmetric surface distance, Normalized surface distance, Boundary intersection over union

## Introduction

Method performance evaluation is the process of assessing how well a method performs in achieving its intended objectives through the analysis of its accuracy, efficiency and reliability under specific conditions. In the field of image analysis spanning applications in (bio)medical imaging, which have been rapidly evolving in the past decade owing to the integration of artificial intelligence, performance evaluation constitutes a cornerstone of every study [1–3]. Metrics serve as proxies for evaluating task performance, and are broadly categorized into *qualitative* and *quantitative*. Qualitative metrics are commonly based on visual inspection and offer focused, direct evaluations of specific tasks, such as clinical acceptability of the automatically generated organ segmentations [4]. However, they often rely on subjective expert judgments, rendering them costly and occasionally impractical or even unfeasible. In contrast, quantitative metrics are swiftly computed, theoretically well-defined, and thus notably objective. While a single metric<sup>1</sup> may not always provide a holistic performance measure, a combination of multiple metrics can provide a solid foundation to aid in decision-making processes, facilitating rapid method prototyping, ablation studies, benchmarking and, generally, the development and validation of novel methodologies.

In the field of medical imaging, a plethora of metrics is currently available. For evaluating image segmentation, which is a fundamental task in biomedical image analysis and an essential prerequisite for a number of clinical applications [5, 6], the well-established metrics, such as the *intersection over union* (IoU), *Dice similarity coefficient* (DSC), *Hausdorff distance* (HD) with its  $p$ -th percentile variants ( $HD_p$ ), *mean average surface distance* (MASD) and *average symmetric surface distance* (ASSD), have been recently complemented by the *normalized surface distance* (NSD) and *boundary intersection over union* (BIOU) [1]. However, not every metric is suitable for evaluating a specific segmentation method or a specific organ undergoing segmentation. Adequate metrics selection is therefore of utmost importance, because it plays a critical role in fostering objective evaluation and reproducibility. Moreover, because it may influence research directions, it should be based on a wide community consensus, for example in the form of metrics selection guidelines [1, 7, 8].

---

<sup>1</sup>In the context of this study, *quantitative metrics* are hereinafter referred to simply as *metrics*.

**Problem identification** Although existing guidelines [1, 7, 8] already identified the problem of *metrics implementation*, represented by the computational translation of the mathematical definition of a selected metric into a computer programming code, it has so far received limited attention and therefore remains an open problem. Incorrect implementation can have considerable ramifications, such as hindering objective comparisons and benchmarking, and distorting method development and decision-making processes, therefore potentially affecting medical device commissioning and introducing bias into medical imaging applications [9, 10]. This is particularly crucial in the current era of rapid research dissemination, where instead of reimplementing baseline methods, research results are commonly compared to those reported in existing studies without explicitly specifying the adopted metrics implementation, but rather with an inherent assumption that metrics implementations across studies are consistent and equivalent throughout the community. Moreover, several open-source tools that implement metrics computation are advocated and adopted in specific areas of biomedical image analysis [1, 7, 8, 11–18], however, their validity has so far not been questioned. If different metrics implementations are used, the conclusions drawn from such comparisons may be biased or even invalid. While the *overlap-based* or *counting metrics*, such as IoU and DSC, are relatively consistently implemented because of their underlying design, *distance-based metrics*, such as HD with  $HD_p$ , MASD, ASSD, NSD and BIoU, lack uniformity across the community because the computation of distances is not trivial.

**Purpose** In this study, we therefore question the assumption of consistency of distance-based metrics, introduce a reference implementation for their computation, and use the reference implementation to systematically analyze and objectively compare existing open-source tools that implement distance-based metrics. Besides adopting the nomenclature and mathematical definitions, we pay homage to the seminal work of *Metrics Reloaded* [1] by naming our study *Metrics Revolutions*<sup>2</sup>, as we hope it will revolutionize the perspective of metrics selection and implementation, and contribute to the evolution of unified metrics design and development within the community.

**Contributions** The main contributions of our study are: (i) we provide a complete collection of open-source tools that implement distance-based metrics computation, (ii) we break down the computation process of each open-source tool to identify and analyze the implementation differences, (iii) we introduce a highly accurate mesh-based reference implementation for distance-based metrics computation that adheres to mathematical definitions, (iv) we design experiments on real-world clinical data, and provide evidence of systematic implementation errors and statistically significant differences among metric scores, obtained by different open-source tools, and (v) we provide recommendations for the medical imaging community related to the appropriate interpretation and usage of open-source tools for distance-based metrics computation.

## Methods

We first present the widely adopted mathematical definitions of the five distance-based metrics (i.e. HD with  $HD_p$ , MASD, ASSD, NSD and BIoU) and their limitations, followed by an analysis of the existing metric selection guidelines. We then introduce the open-source tools for distance-based metrics computation, and describe our reference implementation `MeshMetrics` that adheres to the revised mathematical definitions. We conclude with a description of the experiments that we performed on real-world clinical data to compare the open-source tools and quantitatively observe their variations in metric score computation.

### Distance-based metrics and their limitations

Initially introduced by Felix Hausdorff in 1914 [19] and popularized by Huttenlocher et al. in 1993 [20], HD represents one of the earliest metrics for evaluating the spatial distance between objects and quantify the underlying dissimilarities. Their seminal work also addresses the challenge of determining the adequate quantile or percentile of HD for the computation of  $HD_p$ . Both HD and  $HD_p$  garnered attention within the medical imaging community as metrics for evaluating the segmentation results owing to their interpretability. As they quantify the largest distance between the boundaries of two segmentations, they offer a straightforward metric interpretation with a well-defined unit, which is in biomedical image analysis typically measured in millimeters. Subsequently, several derivative metrics akin to HD have emerged including MASD [21] and ASSD [22], which are less sensitive to segmentation outliers, therefore offering a more generalized measure of proximity between the two boundaries. On the other hand, the recently introduced NSD [12] and BIoU [23] are bounded within the range of 0 to 1 and therefore lack traditional distance units, but are according to their computation and interpretation classified under distance-based metrics.

**Mathematical definitions** In their straightforward application, all distance-based metrics compare two segmentations  $A$  and  $B$ , which are, in the context of biomedical image analysis, commonly represented as binary segmentation masks  $A_{\mathcal{M}}$  and  $B_{\mathcal{M}}$ . The mathematical definitions of HD (and  $HD_p$ ), MASD and ASSD are based on two finite sets  $A_{\mathcal{P}} = \{a_1, a_2, \dots, a_N\}$  and  $B_{\mathcal{P}} = \{b_1, b_2, \dots, b_M\}$ , which represent clouds of  $N$  and  $M$  points describing the surfaces of  $A_{\mathcal{M}}$  and  $B_{\mathcal{M}}$ , respectively, and are used to compute distances between these two sets (Fig. 3, cf. **PointDef**). Assuming that  $D_{AB}$  denotes the set of one-directional (asymmetric) distances of points  $a \in A_{\mathcal{P}}$  to  $B_{\mathcal{P}}$ ,

<sup>2</sup> *The Matrix (franchise)*: Wikipedia, The Free Encyclopedia; [https://en.wikipedia.org/w/index.php?title=The\\_Matrix\\_\(franchise\)](https://en.wikipedia.org/w/index.php?title=The_Matrix_(franchise))

and that  $[D_{AB}]_p$  denotes the  $p$ -th percentile of  $D_{AB}$ , then  $HD_p$  measures the largest among the bi-directional (symmetric) percentile distances  $[D_{AB}]_p$  and  $[D_{BA}]_p$ , i.e.  $HD_p = \max([D_{AB}]_p, [D_{BA}]_p)$ . The 100-th percentile variant  $HD_{100}$ , or simply HD, can be simply computed by replacing the percentile calculation with the maximum over both sets, i.e.  $HD = \max(\max(D_{AB}), \max(D_{BA}))$ . Other variants are less sensitive to outliers in the form of noise and artifacts [9, 24], and the 95-th percentile variant  $HD_{95}$  is the most established one. Often referred to as the average surface distance, MASD computes the mean of the two average distances of sets  $D_{AB}$  and  $D_{BA}$ , while ASSD computes the mean of the union of both sets  $D_{AB}$  and  $D_{BA}$ . On the other hand, NSD and BIoU are defined using the boundary representation of the segmentation masks, where we use the term *boundary* in a context agnostic to the dimensionality, referring to a contour line in two dimensions (2D) and a surface in three dimensions (3D). Also referred to as the (normalized) surface Dice, NSD quantifies the overlap of the two segmentation boundaries,  $A_B$  and  $B_B$ , within a specified margin of error, i.e. a user-defined parameter  $\tau$ . A region  $A_B^{(\pm\tau)}$  is first defined both inward ( $-\tau$ ) and outward ( $+\tau$ ) of boundary  $A_B$ , and NSD is then computed as the ratio of  $B_B$  within  $A_B^{(\pm\tau)}$ , and vice versa, against the total size of both boundaries, represented by the contour circumference in 2D and surface area in 3D. Finally, BIoU enhances the sensitivity to boundary segmentation errors compared to the plain IoU or DSC, which are often saturated for bulk overlaps between two large segmentations. A region  $A_B^{(-\tau)}$  is first defined only inward ( $-\tau$ ) of  $A_B$ , and BIoU is then computed by measuring the intersection of  $A_B^{(-\tau)}$  and  $B_B^{(-\tau)}$  over their union.

**Limitations** The mathematical definitions of HD with  $HD_p$ , MASD and ASSD therefore rely on distances between the point sets describing the boundaries of  $A$  and  $B$ , which are in the discrete image space represented by line polygons in 2D and surface meshes in 3D. However, these point sets lack the complete information regarding the segmentation boundaries, making them a lossy representation of the segmentation masks. The point-based definitions of distance-based metrics inherently neglect the spatial distribution of points across the boundaries, thus assuming that they are distributed uniformly. However, ensuring that each point used for distance calculation, also referred to as the *query point*, corresponds to boundary regions of uniform size is practically challenging, and introduces a bias in metrics computation. For an unbiased computation, we need to take into account also the size of the boundary element, represented by the length of the line segment in 2D and the area of the (triangular) surface element in 3D, at each query point. The distances calculated between query points and the opposing boundary need to be then weighted by the corresponding boundary element sizes, as supported by both the theoretical perspectives and the obtained experimental results (Fig. A1).

## Metric selection guidelines

Several comprehensive examinations of metrics focused on the evaluation of image segmentation and corresponding guidelines for their selection have been proposed so far [1, 7, 8, 25], along with specific recommendations for distance-based metrics usage.

**Taha and Hanbury (2015)** In 2015, Taha and Hanbury [7] conducted correlation analyses among different metrics, revealing that HD exhibits little correlation with others, thus providing distinct insights into the segmentation (dis)similarity. They recommended the usage of HD, particularly when the overall segmentation accuracy is of paramount importance. In cases where sensitivity to outliers is not desired, employing  $HD_p$  or MASD was advised.

**Müller et al. (2022)** A similar investigation was undertaken by Müller et al. in 2022 [8], who identified several common pitfalls in the research community, including *incorrect metrics implementation*. To rectify these issues and enhance future research quality, they proposed several guidelines, the most relevant to our work being their advocacy for open access to evaluation scripts via platforms like GitHub<sup>3</sup> or Zenodo<sup>4</sup>.

**Maier-Hein et al. (2022) – Metrics Reloaded** The most comprehensive effort to date on metrics selection guidelines for a wide range of medical imaging tasks, including classification, detection and semantic/instance segmentation, was published by Maier-Hein et al. in 2024 [1], although available on arXiv since 2022 [26]. This initiative was originally established within the Medical Image Computing and Computer-Assisted Intervention Society as a Special Interest Group (SIG) on the topic of Biomedical Image Analysis Challenges<sup>5</sup>, but since its inception, the focus of the SIG has shifted from challenges to evaluation metrics. By a collaborative consortium of medical imaging researchers utilizing the Delphi process [27], the pitfalls related to problem categorization, metrics selection and application were first identified [9], and followed by the release of comprehensive metrics selection guidelines packaged under the ingenious name of *Metrics Reloaded*<sup>2</sup>. These guidelines, also devised as an online tool<sup>6</sup> to help researchers select relevant validation metrics, comprise mathematical definitions of commonly used metrics in biomedical image analysis, combined with unified nomenclature, properties and limitations. Among the identified pitfalls, the most relevant to our work is the *inadequate metrics implementation*, where the authors highlighted that the method used for extracting the segmentation boundary, which is an integral part of all distance-based metrics, is not unified across different tools and can thus influence the resulting metric scores.

<sup>3</sup><https://github.com/>

<sup>4</sup><https://zenodo.org/>

<sup>5</sup><https://miccai.org/index.php/special-interest-groups/challenges/>

<sup>6</sup><https://metrics-reloaded.dkfz.de/>

**Drukker et al. (2024) – MIDRC-MetricTree** The most recent work on metrics selection was published by Drukker et al. [25], who introduced an online decision tree-based metrics recommendation tool named *MIDRC-MetricTree*<sup>7</sup>. While this study expands on the scope of *Metrics Reloaded* by covering tasks such as time-to-event analysis and estimation tasks, it does not contribute new insights relevant to metrics implementation pitfalls.

## Open-source tools

We conducted a web search for open-source tools that provide distance-based metrics computation with the following inclusion criteria: (i) the tool has to implement at least one of the distance-based metrics (i.e. HD, HD<sub>p</sub>, MASD, ASSD, NSD or BIoU), (ii) the tool has to support computation in 3D, and (iii) the tool has to be coded either in C++ or Python programming language.

**List of open-source tools** The search resulted in the following 11 open-source tools (listed in alphabetical order):

- **Anima** – Initially proposed for the evaluation of multiple sclerosis lesion segmentation method [11].
- **EvaluateSegmentation** – Released by Taha and Hanbury concurrently with their work [7].
- **Google DeepMind** – Introduced alongside the study that proposed NSD [12].
- **MedPy** – A general-purpose toolbox for image processing [13].
- **Metrics Reloaded** – Includes implementations of all metrics analyzed within *Metrics Reloaded* [1].
- **MISeval** – Released by Müller et al. concurrently with their work [8].
- **MONAI** – Widely recognized in biomedical image analysis, initially supported by NVIDIA [14].
- **Plastimatch** – Established for biomedical image registration and segmentation [15], utilized within *SlicerRT*, a radiotherapy research extension of the open-source software *3D Slicer* [28].
- **pymia** – Used for deep learning-based biomedical image analysis, primarily proposed for data handling and evaluation [16].
- **seg-metrics** – Recently released for segmentation metrics calculation [17].
- **SimpleITK** – Multi-dimensional image analysis based on the *Insight Toolkit* (ITK) [18].

Table 1 presents detailed information of all open-source tools, including the programming language in which they are implemented and the set of distance-based metrics they support. We also provide information on the versions and exact commit hashes of the repositories used for our experiments so as to ensure their reproducibility, which correspond to the latest updates for each tool available as of February 2024. In addition to 3D computations, all tools also support computation in 2D. The tools differ in various aspects, such as their popularity within the community, inception date, maintenance level, programming language, customization options, etc. It has to be noted that their development trajectories are not isolated but rather interconnected, with older tools influencing the design of newer ones. In fact, certain segments of the programming code may even be identical, for example, the implementation of HD, HD<sub>p</sub> and NSD of *pymia* is directly adapted from *Google DeepMind*, along with a proper attribution. However, for MASD, *pymia* uses the average HD implementation from *SimpleITK* (i.e. *pymia* uses two different boundary extraction methods, as shown in Fig. 2).

**Properties of open-source tools** All open-source tools can be decomposed into two distinct steps: (1) the method for boundary extraction that converts binary segmentation masks into sets of query points, and (2) the implementation of mathematical definitions for calculating the metric scores. The first major variation among different open-source tools is related to boundary extraction. The seminal work of Huttenlocher et al. [20] can be considered a foundation for all modern implementations, however, it does not explicitly describe how to obtain query points from binary segmentation masks. Based on the figures in their study, it can be concluded that they probably used a boundary extraction algorithm, such as the Canny edge detector, to define query points used for HD computation. The ambiguity around the boundary extraction method has led to a large diversity in practical implementations, ranging from using all foreground elements as query points to using different boundary extraction methods. While this is understandable given the historical context, it considerably impacts the computed metric scores, as it hinders the interpretation, objective comparison and evaluation of the results in studies using distance-based metrics. The second major variation among the implementations of different open-source tools pertains to the application of mathematical definitions to real-world scenarios, which are inevitably subjected to discretization artifacts. Because the study of Huttenlocher et al. [20] does not address such practical challenges, existing open-source tools exhibit variability in this aspect as well.

## Reference implementation

To mitigate the variations identified for existing open-source tools while demanding highly accurate metric scores, we propose a mesh-based reference implementation, named **MeshMetrics**, for computing distance-based metrics that adheres to their revised mathematical definitions and incorporates boundary element size weighting [12]. Considering

<sup>7</sup><https://www.midrc.org/performance-metrics-decision-tree/>

---

**Algorithm 1** Distance calculation between two segmentation masks.

---

```
1: Input: Segmentation masks  $A$  and  $B$ .
2: Output: Sets of distances  $D_{AB}$  and  $D_{BA}$ , and sets of corresponding boundary element sizes  $S_A$  and  $S_B$ .
3: Step 1: Extract boundary representation:
4: if 2D then
5:   Use discrete flying edges algorithm to convert masks  $A$  and  $B$  to line polygons.
6: else if 3D then
7:   Use discrete marching cubes algorithm to convert masks  $A$  and  $B$  to triangle meshes.
8: end if
9: Upsample the meshes to reduce the size of boundary elements while preserving the overall mesh circumference
   in 2D or volume in 3D.
10: Step 2: Calculate distances and boundary element sizes:
11: for each boundary element  $e_i \in A$  do
12:   if 2D then
13:     Calculate the midpoint of line segment  $e_i$  and use it as a query point  $q_i$ .
14:   else if 3D then
15:     Calculate the centroid of mesh triangle  $e_i$  and use it as a query point  $q_i$ .
16:   end if
17:   Calculate the distance,  $d_i$ , from  $q_i$  to the opposing boundary.
18:   Record the size of the corresponding boundary element  $e_i$  as  $s_i$ .
19:   Append  $d_i$  to  $D_{AB}$  and  $s_i$  to  $S_A$ .
20: end for
21: Repeat Step 2 for each  $e_j \in B$  to obtain  $D_{BA}$  and  $S_B$ .
22: Step 3: Sort sets  $\{D_{AB}, S_A\}$  and  $\{D_{BA}, S_B\}$ :
23: for each  $\{D_{AB}, S_A\}$  and  $\{D_{BA}, S_B\}$  as  $\{D, S\}$  do
24:   if 2D or 3D then
25:     Sort the distances in  $D$  in ascending order.
26:     Apply the same order to boundary element sizes in  $S$ .
27:   end if
28: end for
29: Return:  $\{D_{AB}, S_A\}$  and  $\{D_{BA}, S_B\}$  for metrics computation.
```

---

the critical importance of accuracy in metrics computation, especially for comparing the open-source tools, we prioritize accuracy over computational efficiency and therefore define the reference implementation in the mesh domain, which avoids the discretization artifacts that are inevitable in the image grid domain, thereby ensuring more accurate results.

**Mesh domain** For our reference implementation, we leverage the fact that distance-based metrics are more elegantly computed in the mesh domain than in the (segmentation) mask domain due to the inherent availability of boundary elements in meshes and the capability to implicitly calculate the distances between a point and a mesh. A necessary condition, that masks can be converted to meshes without any information loss, is met because the mesh representation can be considered a generalization of a binary mask representation: every 2D or 3D binary mask can be converted to a 2D or 3D mesh without loss of information, whereas the reverse process may not always be possible due to discretization errors introduced by the grid-like representation of the mask domain. Additionally, every mesh created from a mask has the property of being watertight, provided the input binary mask does not include foreground elements on the mask edges, which can be ensured by mask zero-padding. In the case the mask includes multiple connected components, the conversion will result in multiple watertight meshes. In the borderline case, when a mesh consists of very small boundary elements, we approach a smooth representation of the contour/surface, thus controlling the effect that finite element discretization has on the measurements. The conversion of binary masks to meshes, often referred to as *isosurface extraction* or simply *meshing*, can be achieved by several robust algorithms (Fig. A2). A widely established method is the *marching squares* algorithm for 2D masks or the *marching cubes* algorithm for 3D masks, which produce a line polygon or a triangle mesh, respectively, that spans between the corresponding vertices.

**Distance calculation** The proposed reference implementation adopts the following three steps for calculating the distances (Algorithm 1): (1) we first extract boundary representations  $A_B$  and  $B_B$  of segmentation masks  $A$  and  $B$  using line polygons for 2D (with *discrete flying edges* algorithm [29]) and triangle meshes for 3D (with *discrete marching cubes* algorithm [30]), and upsample the resulting representation so that the discretization effect of the original image grid is further suppressed [31], (2) we then place query points  $A_Q$  and  $B_Q$  at the boundary element centerpoints, represented by the midpoints of the line segments in 2D and the centroids of the mesh triangles in 3D, and compute for each query point the distance from  $A$  to  $B$  and the corresponding boundary element size in  $A_B$ , and vice-versa, (3) we finally sort each set of computed distances in ascending order and apply the same order to the corresponding set of boundary element sizes.

**MeshMetrics** The proposed reference implementation for distance-based metrics computation, **MeshMetrics**, utilizes the mesh representations of segmentation masks, follows Algorithm 1 for distance calculation, and incorporates the resulting ordered sets of distances and boundary element sizes with the revised equations from Fig. 3 (cf. **MeshMetrics** vs. **PointDef**) to obtain HD with  $\text{HD}_p$ , MASD, ASSD, NSD and BIoU. While the proposed approach does not affect the computation of HD, because the 100-th percentile equals the maximal value of a set, it considerably impacts  $\text{HD}_p$ , which is computed from the indices that correspond to the  $p$ -th percentile on the sets of normalized cumulative boundary element sizes. To compute MASD and ASSD, the original averaging on the sets of distances is augmented by the weighted averaging on the sets of boundary element sizes. Furthermore, the computation of NSD is in agreement with its mathematical definition that already considers boundary element sizes, while the computation of BIoU involves accurately calculating the signed distance field from both meshes using an image grid that is five times denser than the original image grid. Both fields are then thresholded by  $\tau$  to generate two volumes, which are subsequently used to compute IoU.

## Quantitative experiments

To quantitatively evaluate the compound effect of variations in boundary extraction methods and mathematical definitions on the resulting metric scores, we designed a series of experiments to assess the accuracy of the 11 open-source tools for distance-based metrics computation, along with edge case handling and computational efficiency analysis.

**Dataset** We devised a real-world dataset of 30 computed tomography (CT) and 30 magnetic resonance (MR) images of the same patients from the radiotherapy planning workflow, where each image is coupled with corresponding 3D segmentations of up to 30 organs-at-risk (OARs) that were individually provided by two clinical experts, resulting in 1,561 pairs of OAR segmentation masks  $A$  and  $B$ . The devised dataset is part of our recently released and publicly available *HaN-Seg dataset*<sup>8</sup>, and its detailed description can be found in our studies on dataset conception [32], multi-modal auto-segmentation [33], inter-observer and inter-modality variability evaluation [34] and computational challenge benchmarking [35]. This dataset was chosen for three key reasons. First, 3D CT and MR images are among the most widely applied modalities in biomedical image segmentation [36]. Second, distance-based metrics, such as HD and especially  $\text{HD}_{95}$ , are commonly used alongside DSC for evaluating the quality of OAR auto-segmentation [37]. Third, OARs in the head and neck region exhibit a complex structure with considerable variations in shape and size [38]. As a result, we were able to devise a realistic and comprehensive evaluation of how the variations in distance-based metrics computation impact the obtained scores.

**Experimental design** In contrast to counting metrics, distance-based metrics rely on distance calculations and therefore require the image grid to be defined in distance units, i.e. with pixel size  $(d_x, d_y)$  or voxel size  $(d_x, d_y, d_z)$ . For our 3D CT and MR images, we conducted experiments for three different voxel sizes: (1) (1.0, 1.0, 1.0) mm, simulating the *vanilla scenario* with isotropic voxels of unit size, (2) (2.0, 2.0, 2.0) mm, a commonly used isotropic voxel size, and (3) (0.5, 0.5, 2.0) mm, a commonly used anisotropic voxel size in the radiotherapy workflow. The experiments were performed according to the following procedure (Fig. 1): (1) for a chosen CT or MR image, the two OAR segmentation masks were first loaded with their original image voxel size, (2) meshing was performed to extract triangle meshes from segmentation masks, (3) mesh rasterization (i.e. voxelization in our 3D case) was performed to obtain each of the three voxel sizes, which were used to compute the distance-based metrics by each of the 11 open-source tools, and (4) meshing was again performed for each voxelized mask to compute the distance-based metrics using our reference implementation **MeshMetrics**. For those metrics that depend on user-defined parameters, i.e. percentile  $p$  for  $\text{HD}_p$ , and boundary margin of error  $\tau$  for NSD and BIoU, we conducted experiments for  $\text{HD}_{p=95}$ ,  $\text{NSD}_{\tau=2\text{mm}}$  and  $\text{BIoU}_{\tau=2\text{mm}}$ , as these values are commonly used by existing studies [1] and offer a good insight into the differences among the tools.

**Evaluation of differences** Comparing different implementations for individual OARs would be challenging due to the disparity of the results, therefore we focus on analyzing the deviations between each open-source tool and **MeshMetrics**, defined as  $\Delta_j = m_{j,i} - m_r$ , where  $m_i$  is the metric score of  $j$ -th open-source tool and  $m_r$  is the reference metric score of **MeshMetrics**. The distance-based metrics can be divided into two groups: (1) absolute metrics (HD with  $\text{HD}_p$ , MASD and ASSD), measured in metric units (i.e. for our case in millimeters, mm), without an upper bound, with a lower score reflecting a greater similarity between two masks, and (2) relative metrics (NSD and BIoU), bounded between 0 and 1, unitless, with a higher score reflecting a greater similarity between two masks. In the context of this analysis, positive  $\Delta_j$  values indicate an *overestimation* of the metric score (i.e. over-pessimistic for absolute and over-optimistic for relative metrics), while negative  $\Delta_j$  values indicate an *underestimation* of the metric score (i.e. over-optimistic for absolute and over-pessimistic for relative metrics). Although both are undesirable, over-optimistic estimates are particularly concerning, as they may lead to incorrect conclusions, especially when compared to metric scores reported in existing studies.

<sup>8</sup><https://doi.org/10.5281/zenodo.7442914>

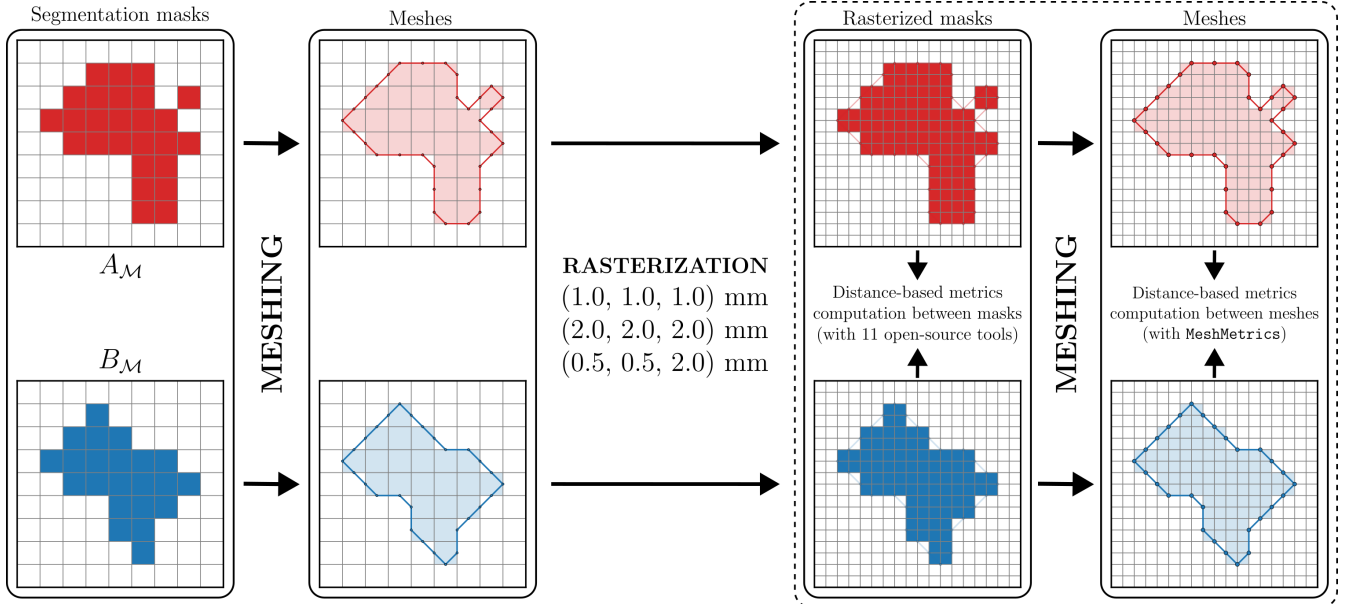


**Fig. 1.** Experimental design for distance-based metrics computation using the 11 open source tools and our reference implementation **MeshMetrics**. Meshes are first generated from original segmentation masks, and then rasterization (voxelization) to three different voxel sizes is applied. The rasterized (voxelized) masks are then used as inputs to open-source tools, and for generating corresponding highly accurate meshes that are used as inputs to **MeshMetrics**.

**Statistical testing** In addition, we searched for statistically significant differences in the distributions of the resulting metric scores across the open-source tools using the paired Wilcoxon signed-rank test with the Bonferroni correction. Considering that the distance-based metrics share the same underlying computational principles and therefore statistical independence cannot be assumed, we applied a conservative Bonferroni adjustment by multiplying the resulting  $p$ -value by the total number of 1,188 comparisons made between all tools, including **MeshMetrics**, and across all distance-based metrics.

**Edge case handling** Proper handling of edge cases is crucial for an objective evaluation. By *edge cases*, we refer to scenarios where one or both inputs, represented by segmentation masks  $A$  and  $B$ , are empty (i.e. contain no foreground pixels/voxels). We systematically analyzed all open-source tools to determine how they handle each of the three possible edge cases: (1) only  $A$  is empty, (2) only  $B$  is empty, and (3) both  $A$  and  $B$  are empty. Additionally, we also verified if the resulting metric scores remain unchanged when the inputs are swapped, i.e. from  $(A, B)$  to  $(B, A)$ .

**Computational efficiency analysis** Although accuracy is the primary focus of metrics evaluation, *computational efficiency* is also important from the perspective that efficient implementations facilitate rapid prototyping, provide real-time feedback and conserve computational resources. To assess the computational efficiency, we focused solely on HD as the only metric that is supported across all open-source tools, and measured the corresponding average execution times for the voxel size of (1.0, 1.0, 1.0) mm. It has to be noted that a substantial disparity in execution times can be attributed to a simple optimization in the form of prior cropping of segmentation masks  $A$  and  $B$  to the smallest bounding box that encompasses both. While this approach may introduce issues for certain counting metrics, it is entirely suitable for distance-based metrics as it can considerably accelerate metric computation, given that foreground elements typically occupy only a relatively small portion of the entire image. Another noteworthy consideration is the calculation of distances involved in metrics computation, which can be recalculated for each individual metric, or calculated only once and then reused across different metrics. Obviously, the latter strategy results in an accelerated simultaneous computation of multiple metrics.

## Results

We systematically analyzed 11 different open-source tools for distance-based metrics computation (Table 1): **Anima** [11], **EvaluateSegmentation** [7], **GoogleDeepMind** [12], **MedPy** [13], **MetricsReloaded** [1], **MISeval** [8], **MONAI** [14], **Plastimatch** [15], **pymia** [16], **seg-metrics** [17] and **SimpleITK** [18] (listed alphabetically). By following the mathematical definitions of distance-based metrics, we designed a highly accurate mesh-based reference implementation, **MeshMetrics**, and used it to validate and compare the open-source tools against OAR segmentation masks  $A$  and  $B$  in the head and neck region, obtained from the radiotherapy planning workflow [32, 34].

**Table 1.** Overview of 11 open-source tools analyzed in this study, indicating the supported distance-based metrics (names are hyperlinked to corresponding publications, commit hashes are hyperlinked to publicly available code repositories). For HD<sub>p</sub>, the checkmark (✓) denotes the support of any percentile, whereas a specific number indicates the implementation of a predefined percentile (e.g. 95-th).

Open-source tool	Details			Distance-based metrics					
	Commit hash	Version	Language	HD	HD <sub>p</sub>	MASD	ASSD	NSD	BIoU
<a href="#">Anima</a> [11]	<a href="#">1df7e44</a>	4.2	C++	✓		✓ <sup>a</sup>	✓ <sup>a</sup>		
<a href="#">EvaluateSegmentation</a> [7]	<a href="#">4cff08d</a>	N/A	C++	✓	95	✓ <sup>b</sup>			
<a href="#">Google DeepMind</a> [12]	<a href="#">ee651c8</a>	0.1	Python	✓	✓	✓ <sup>c</sup>	✓ <sup>c</sup>	✓	
<a href="#">MedPy</a> [13]	<a href="#">54bb190</a>	0.4.0	Python	✓	95	✓ <sup>d</sup>			
<a href="#">Metrics Reloaded</a> [1]	<a href="#">b3a3715</a>	0.1.0	Python	✓	✓	✓	✓	✓	✓
<a href="#">MISeval</a> [8]	<a href="#">f4695ce</a>	1.2.2	Python	✓ <sup>e</sup>					
<a href="#">MONAI</a> [14]	<a href="#">865972f</a>	1.3.0	Python	✓	✓	✓ <sup>f</sup>	✓ <sup>f</sup>	✓	
<a href="#">Plastimatch</a> [15]	<a href="#">581c7692</a>	1.9.4	C++	✓ <sup>g</sup>	95 <sup>g</sup>	✓ <sup>g</sup>			
<a href="#">pymia</a> [16]	<a href="#">c9821e0</a>	0.3.2	Python	✓	✓	✓ <sup>h</sup>		✓	
<a href="#">seg-metrics</a> [17]	<a href="#">df9a231</a>	1.1.6	Python	✓	95		✓ <sup>i</sup>		
<a href="#">SimpleITK</a> [18]	<a href="#">42ce27d</a>	2.3.1	Python	✓		✓ <sup>j</sup>			
<b>MeshMetrics</b> (proposed)	<a href="#">357b19c</a>	0.1	Python	✓	✓	✓	✓	✓	✓

<sup>a</sup> *Anima*: Metric name is `ContourMeanDistance` for MASD, and `SurfaceDistance` for ASSD. <sup>b</sup> *EvaluateSegmentation*: Metric name is `ASD` for MASD. <sup>c</sup> *GoogleDeepMind*: Function `compute_average_surface_distance` returns the two directed average distances and we take their mean to obtain MASD, while function `compute_surface_distances` returns vectors of distances and corresponding boundary element sizes that we use to calculate ASSD. <sup>d</sup> *MedPy*: Metric name is `ASD` for MASD. <sup>e</sup> *MISeval*: Function `calc.SimpleHausdorffDistance` only works for 2D, therefore we use `calc.AverageHausdorffDistance` to calculate HD in 3D, which is the implementation of HD<sub>100</sub> despite its name. <sup>f</sup> *MONAI*: We use `compute_average_surface_distance` with argument `symmetric` set to `False` to calculate MASD, and `compute_average_surface_distance` with argument `symmetric` set to `True` to calculate ASSD. <sup>g</sup> *Plastimatch*: Metric name is `Hausdorff distance (boundary)` for HD, `Percent (0.95) Hausdorff distance (boundary)` for HD<sub>95</sub>, and `Avg average Hausdorff distance (boundary)` for MASD. <sup>h</sup> *pymia*: Metric name is `AverageDistance` for MASD. <sup>i</sup> *seg-metrics*: Metric name is `msd` for ASSD. <sup>j</sup> *SimpleITK*: We use `GetAverageHausdorffDistance` method of the `HausdorffDistanceImageFilter` class to calculate MASD.

### Commentary:

As observed from the remarks, there is a considerable ambiguity surrounding the nomenclature used for MASD and ASSD. While we adopt the nomenclature from the *Metrics Reloaded* framework [1], it is important to acknowledge that various names are used for the same or similar metrics throughout the literature. To accommodate this, we took an inclusive approach, incorporating metrics from open-source tools with different naming conventions as long as there was a strong resemblance in their mathematical definitions, or a possibility that a less experienced user may confuse them with MASD or ASSD. For example, MASD is often referred to simply as ASD by *EvaluateSegmentation* and *MedPy*, or average HD by *Plastimatch* and *SimpleITK*. It is worth noting that average HD is inconsistently defined in the literature – definitions using both the maximum [7, 8] and the mean [39] of the average distances are found, sometimes even from the same authors. Some tools use a less common nomenclature, such as `ContourMeanDistance` and `SurfaceDistance` used by *Anima* that we compare to MASD and ASSD, respectively. Additionally, *MONAI* provides a function to compute ASSD but includes an option to set the `symmetric` argument to `False`. An experienced user may recognize that this function returns the average directed distance, but a less experienced user may easily misinterpret it as MASD. For this reason, we include it in our comparison but advise caution when interpreting these results.

It has to be noted that a distinct similarity exists for two pairs of open-source tools: *Google DeepMind* and *pymia*, as well as *Metrics Reloaded* and *MONAI*, which differ only in their implementation of MASD. In fact, *pymia* contains a direct copy of code sections from *Google DeepMind*, meaning that any code modifications in *Google DeepMind* will not be reflected in *pymia*. In contrast, *Metrics Reloaded* has been made available on the GitHub repository of the *Project MONAI* [14], but both tools are coded independently without sharing any high level code. As a result, we also treat *Metrics Reloaded* and *MONAI* as two separate open-source tools.

## Conceptual analysis

A detailed analysis of open-source tools revealed notable differences in the applied boundary extraction methods (Fig. 2) and metrics calculation strategies (Fig. 3).

**Variations in boundary extraction** A critical pitfall in the implementation of distance-based metrics is boundary extraction [1, 9] (Fig. 2), where the first issue is the foreground- vs. boundary-based calculation dilemma. Among the 11 open-source tools, *EvaluateSegmentation* and *SimpleITK* are the only two that omit the boundary extraction step and calculate distances between all mask foreground elements instead, using the pixel/voxel centers as query points. The authors of *EvaluateSegmentation* even proposed several optimization strategies to improve the computational efficiency, such as excluding intersecting elements because their distances are always zero [40]. *Plastimatch* is the only tool that returns both foreground- and boundary-based calculations, while other tools support boundary-based calculations only. The most frequently employed boundary extraction method is utilized by *Anima*, *MedPy*, *Metrics Reloaded*, *MISeval*, *MONAI* and *Plastimatch*, and involves morphological erosion using a



square-connectivity structural element, while `seg-metrics` uses a full-connectivity structural element. Conversely, `GoogleDeepMind` and `pymia`<sup>9</sup> employ a strategy where the image grid is shifted by half a pixel/voxel size, and incorporate the calculation of boundary element sizes, i.e. the lengths of line segments in 2D and areas of surface elements in 3D. As already explained, `EvaluateSegmentation` computes distances solely for non-overlapping elements [40], while `SimpleITK` computes distances for all foreground elements. Differently from all the 11 open-source tools, our reference implementation `MeshMetrics` adopts a meshing boundary extraction strategy by using *discrete flying edges* in 2D and *discrete marching cubes* in 3D.

**Variations in metrics calculation** Among all distance-based metrics, HD is the only one that is, apart its sensitivity to the boundary extraction method, straightforward to implement (Fig. 3). The remaining metrics, i.e.  $HD_p$ , MASD, ASSD, NSD and BioU, are more complex to compute in the discretized space due to their reliance on distance distributions, making their practical implementations more intricate than their mathematical definitions imply:

- **HD=HD<sub>100</sub>** – This metric is the only one that is mathematically well-defined even in the discretized space because it reports the maximal distance of the maximum of each directed distance, i.e. from  $A$  to  $B$  and from  $B$  to  $A$ . The implementation is consistent across all open-source tools, except for `MISeval`, which does not account for pixel/voxel size when computing the Euclidean distance transform but assumes an isotropic grid of unit size.
- **HD<sub>p</sub>** – First defined by Huttenlocher et al. [20] as the maximum of both directed percentile distances, its calculation requires sorting a set of distances  $D_{AB}$  of cardinality  $N$  in ascending order and selecting the value at position  $(p/100) \cdot N$  (rounded to the nearest integer). This approach, denoted as  $[D_{AB}]_p$ , is employed by `Metrics Reloaded` and `MONAI`, but is only valid when the query points are uniformly distributed across the boundary. To address this limitation, `GoogleDeepMind`, `pymia` and `MeshMetrics` adopt a more general approach that accounts for the size of boundary elements. Other variations include the calculation of percentiles on the union of both directed sets of distances, which is implemented by `seg-metrics`, `MedPy` and `EvaluateSegmentation`. All these tools calculate the maximal value between the two directed percentile distances, while `Plastimatch` reports the average of the two instead. While `EvaluateSegmentation` incorporates optimization strategies for distance-based metrics [40], these strategies can only be applied to HD=HD<sub>100</sub> and do not generalize to HD<sub>p</sub>, therefore producing skewed, biased and non-deterministic results due to distorted distance distributions.
- **MASD** – Among different approaches, the most common one is applied by `EvaluateSegmentation`, `Metrics Reloaded`, `Plastimatch`, `pymia` and `SimpleITK` that sum the distances in each directed set and divide the sum by the number of query points in that set, and finally average the two results. Conversely, `Anima` reports the maximum of both directed averages, `MONAI` and `MedPy` report only the directed average from  $A$  to  $B$  but not from  $B$  to  $A$ , while `GoogleDeepMind` adds an extra layer of complexity by introducing weighted averaging based on the boundary element sizes.
- **ASSD** – Among two main approaches, `Anima`, `Metrics Reloaded`, `MONAI` and `seg-metrics` sum both sets of distances and divide the sum by the total number of distances in both sets, while `GoogleDeepMind` applies weighted averaging based on the boundary element sizes.
- **NSD** – Although the authors of `GoogleDeepMind`, who proposed NSD, explicitly emphasized the importance of the boundary element size for accurate NSD computation [12], `Metrics Reloaded` and `MONAI` use a point-based approach by counting the number of distances below a threshold  $\tau$ , and dividing the count by the total number of distances. In contrast, `GoogleDeepMind` and `pymia` sum the boundary element sizes with the corresponding distances below  $\tau$ , and then divide the sum by the total size of all boundary elements.
- **BioU** – Supported only by `Metrics Reloaded`, this metric operates as a hybrid between counting and distance-based metrics, concentrating on the overlap of boundary regions rather than the whole segmentation mask. While the mathematical definitions remain consistent, `Metrics Reloaded` performs calculations on a discretized grid but with a flaw in its programming code: pixel/voxel size is not properly accounted for.

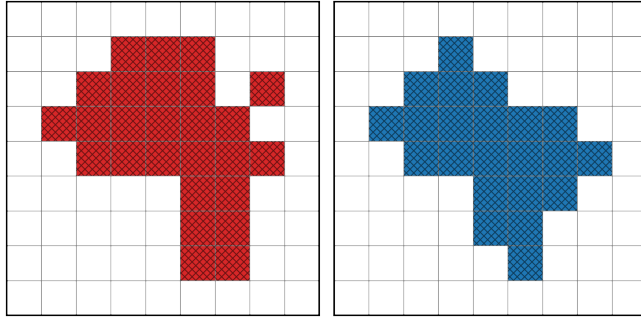
## Quantitative analysis

Computations of all distance-based metrics on 1,561 pairs of OAR segmentation masks from the *HaN-Seg dataset* [32, 34] were performed for three different voxel sizes of (1.0, 1.0, 1.0), (2.0, 2.0, 2.0) and (0.5, 0.5, 2.0) mm. The results are reported in Fig. 4 and Table A1, revealing notable differences in all metric scores for all open-source tools against our reference implementation `MeshMetrics`. The results obtained by stratifying OARs into groups of small, midsize, large and tubular (Fig. A3) are presented in Table A2.

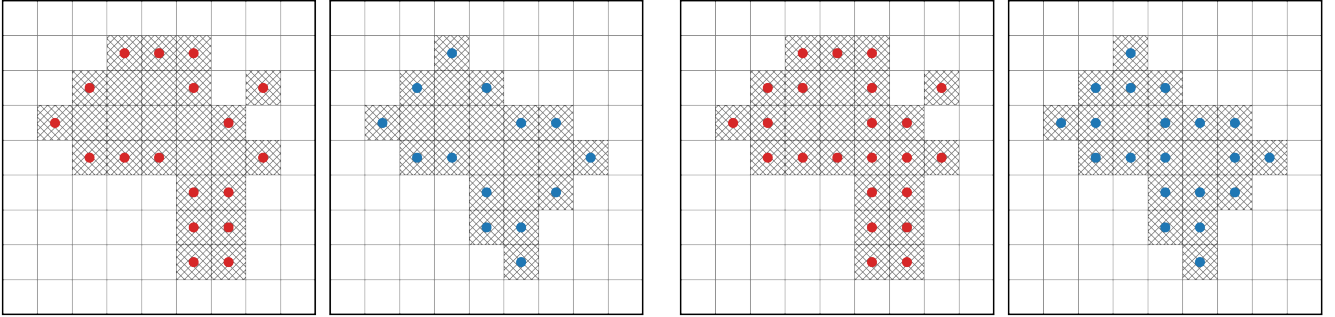
**Statistical testing** The results (Fig. A4) revealed that all open-source tools exhibit statistically significant differences when compared to `MeshMetrics`, with the exception of `MedPy` and `MONAI` for MASD on the anisotropic voxel size. Additionally, statistically significant differences were observed among each pair of open-source tools, with the exception of HD, which is less variable in its mathematical definitions and less sensitive to boundary extraction due to its maximum value statistics.

---

<sup>9</sup>Note that the implementation of `pymia` is based on `GoogleDeepMind`.

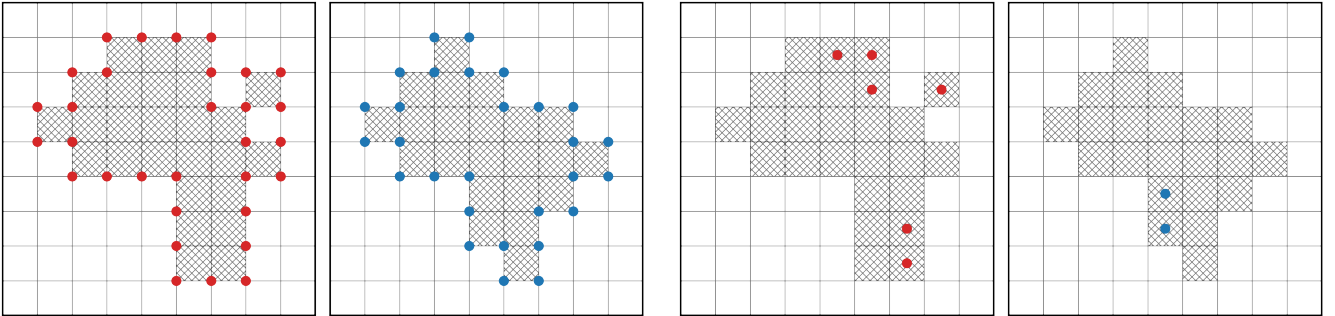


(a) Example segmentation masks  $A$  and  $B$ .



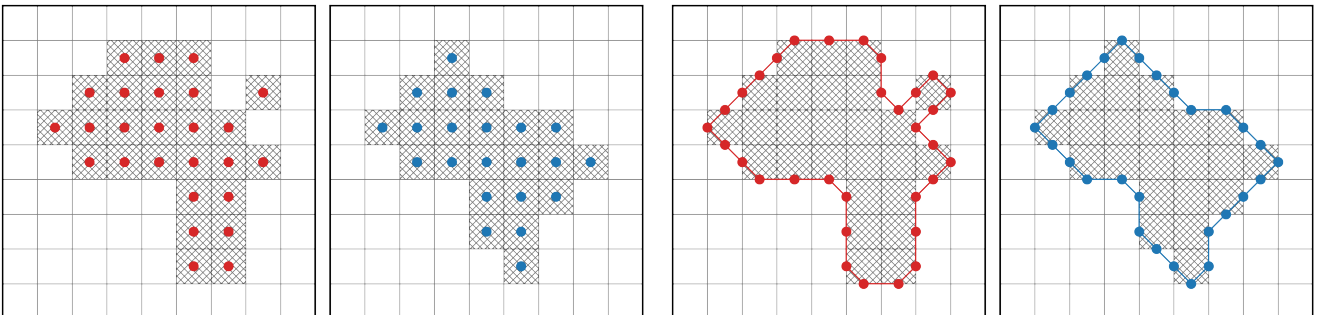
(b) *Anima*, *MetricsReloaded*, *MONAI*, *Plastimatch*, *MedPy*, *MISeval*: The boundary mask is generated by subtracting the eroded binary mask (using a  $3 \times 3$  square-connectivity structuring element) from the original binary mask.

(c) *seg-metrics*: The boundary mask is generated by subtracting the eroded binary mask (using a  $3 \times 3$  full-connectivity structuring element) from the original binary mask.



(d) *Google DeepMind*, *pymia*: Correlation between the segmentation mask and a  $2 \times 2$  non-zero kernel is computed and thresholded to retain positive elements smaller than the kernel sum, which shifts the image grid by half a pixel size. Note that *pymia* uses this algorithm for  $HD$ ,  $HD_p$  and  $NSD$ .

(e) *EvaluateSegmentation*: Distances are calculated solely for non-overlapping pixels without extracting the boundary. This tool is based on a foreground-based calculation, but utilizes several optimization tricks [40].



(f) *SimpleITK*, *pymia*: Distances are calculated for all foreground pixels without extracting the boundary. Note that *pymia* uses this algorithm for  $MASD$ .

(g) *MeshMetrics*: Query points are extracted by a meshing algorithm (e.g. *discrete flying edges* or *discrete marching cubes*).

**Fig. 2.** Overview of the boundary extraction methods used by the 11 open-source tools and our reference implementation *MeshMetrics*. All methods are demonstrated using 2D examples, but can be seamlessly extended to 3D.

General definitions	
$A_{\mathcal{M}} \rightarrow A_{\mathcal{P}} = \{a_1, a_2, \dots, a_N\}$ $d_{a,1} = \min_{b \in B_{\mathcal{P}}} \ a_1 - b\ _2$ $D_{AB} = \{d_{a,1}, \dots, d_{a,N}\}$ ; where: $d_{a,1} \leq \dots \leq d_{a,N}$ $S_A = \{s_{a,1}, \dots, s_{a,N}\}$ , $ S_A  = \sum_{n=1}^N s_{a,n}$ $n_p = \min_x \left\{ \sum_{n=1}^x s_{a,n} \geq \frac{p}{100} \cdot  S_A  \right\}$ $n_{\tau} = \max_x \{d_{a,x} \leq \tau\}$	$B_{\mathcal{M}} \rightarrow B_{\mathcal{P}} = \{b_1, b_2, \dots, b_M\}$ $d_{b,1} = \min_{a \in A_{\mathcal{P}}} \ b_1 - a\ _2$ $D_{BA} = \{d_{b,1}, \dots, d_{b,M}\}$ ; where: $d_{b,1} \leq \dots \leq d_{b,M}$ $S_B = \{s_{b,1}, \dots, s_{b,M}\}$ , $ S_B  = \sum_{m=1}^M s_{b,m}$ $m_p = \min_x \left\{ \sum_{m=1}^x s_{b,m} \geq \frac{p}{100} \cdot  S_B  \right\}$ $m_{\tau} = \max_x \{d_{b,x} \leq \tau\}$

Hausdorff distance, HD	Boundary intersection over union, BIoU
<u>PointDef</u> , MeshMetrics, all tools <sup>a</sup>  $\max(\max(D_{AB}), \max(D_{BA}))$	<u>PointDef</u> , MeshMetrics, Metrics Reloaded <sup>c</sup>  $\frac{ A_B^{(-\tau)} \cap B_B^{(-\tau)} }{ A_B^{(-\tau)} \cup B_B^{(-\tau)} }$
$p$ -th percentile of Hausdorff distance, HD <sub>p</sub>	Mean average surface distance, MASD
<u>PointDef</u> , Metrics Reloaded, MONAI  $\max([D_{AB}]_p, [D_{BA}]_p)$	<u>PointDef</u> , Metrics Reloaded, Plastimatch, pymia, SimpleITK, EvaluateSegmentation <sup>b</sup>  $\frac{1}{2} \left( \frac{\sum_{n=1}^N d_{a,n}}{N} + \frac{\sum_{m=1}^M d_{b,m}}{M} \right)$
MeshMetrics, Google DeepMind, pymia  $\max(d_{a,n_p}, d_{b,m_p})$	MeshMetrics, Google DeepMind  $\frac{1}{2} \left( \frac{\sum_{n=1}^N d_{a,n} \cdot s_{a,n}}{ S_A } + \frac{\sum_{m=1}^M d_{b,m} \cdot s_{b,m}}{ S_B } \right)$
seg-metrics, MedPy, EvaluateSegmentation <sup>b</sup>  $[D_{AB} \cup D_{BA}]_p$	Anima  $\max \left( \frac{\sum_{n=1}^N d_{a,n}}{N}, \frac{\sum_{m=1}^M d_{b,m}}{M} \right)$
Plastimatch  $\frac{1}{2} ([D_{AB}]_p + [D_{BA}]_p)$	MONAI, MedPy  $\frac{\sum_{n=1}^N d_{a,n}}{N}$
Average symmetric surface distance, ASSD	Normalized surface distance, NSD
<u>PointDef</u> , Anima, Metrics Reloaded, MONAI, seg-metrics  $\frac{\sum_{n=1}^N d_{a,n} + \sum_{m=1}^M d_{b,m}}{N + M}$	<u>PointDef</u> , Metrics Reloaded, MONAI  $\frac{N_{\tau} + M_{\tau}}{N + M}$
MeshMetrics, Google DeepMind  $\frac{\sum_{n=1}^N d_{a,n} \cdot s_{a,n} + \sum_{m=1}^M d_{b,m} \cdot s_{b,m}}{ S_A  +  S_B }$	MeshMetrics, Google DeepMind, pymia  $\frac{ A_B \cap B_B^{(\pm\tau)}  +  B_B \cap A_B^{(\pm\tau)} }{ S_A  +  S_B } = \frac{\sum_{n=1}^{n_{\tau}} s_{a,n} + \sum_{m=1}^{m_{\tau}} s_{b,m}}{ S_A  +  S_B }$

<sup>a</sup> MISEval does not take into account the pixel/voxel size when computing distances. <sup>b</sup> The calculation of EvaluateSegmentation is non-deterministic. <sup>c</sup> Metrics Reloaded does not take into account the pixel/voxel size when computing distances.

**Fig. 3.** Mathematical definitions of distance-based metrics as adopted by the point-based definition PointDef, different open-source tools, and our reference implementation MeshMetrics.

**Edge case handling** The results (Table A3) revealed considerable variability across all open-source tools. While most return *not a number* (NaN), infinite values, large integers or error messages, we encountered irregularities in edge case handling pertaining to GoogleDeepMind for MASD, MISEval for HD, MONAI for HD, Plastimatch for HD and MASD, and pymia for NSD. Swapping the inputs caused asymmetry in the results pertaining to EvaluateSegmentation for HD<sub>95</sub> and MASD due to the non-deterministic calculation, and MedPy and MONAI for MASD due to reporting the average *directed* distance.

**Computational efficiency analysis** The results (Fig. A5) revealed substantial differences in the median HD execution times, spanning two orders of magnitude. Overall, the most computationally efficient tool is Google

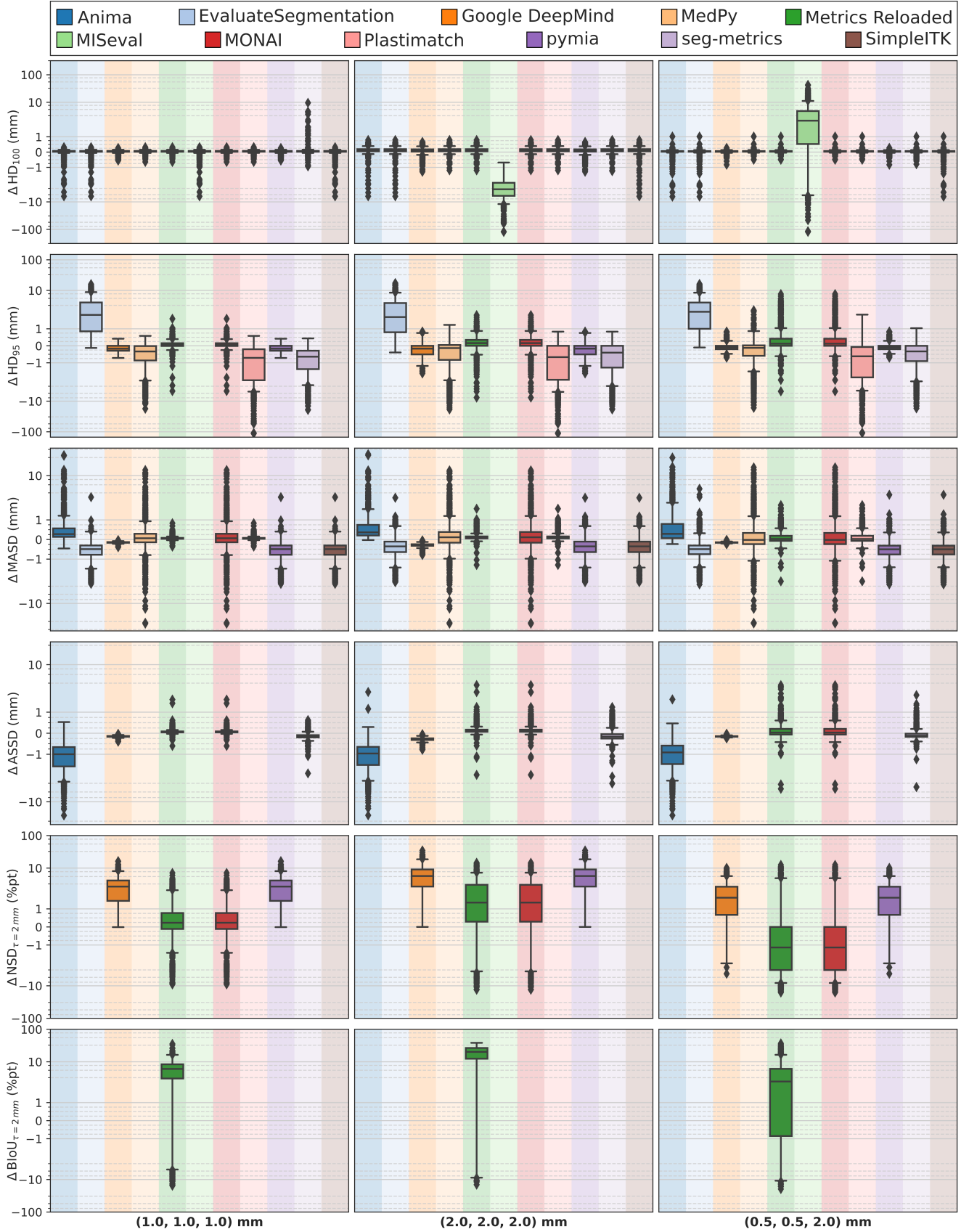


**Fig. 4.** The differences ( $\Delta$ ) in the distance-based metrics, as obtained by each open-source tool against the reference implementation *MeshMetrics* on 1,561 pairs of OAR segmentation masks, reported for two isotropic and one anisotropic voxel size in the form of box-plots. Note that a linear scale is applied for values within the interval  $[-1, 1]$  and a symmetric logarithmic scale for values outside this interval to better visualize both smaller and larger differences.

DeepMind, followed by MONAI. Despite not being primarily optimized for computational efficiency, MeshMetrics ranks third based on the median execution time across all OAR categories.

## Discussion

Distance-based metrics are often referred to as *boundary-based*, a concept reflecting their underlying design and adequacy when compared to foreground-based calculations. For instance, for two large segmentations with a substantial overlap, foreground-based calculations consistently yield smaller values for  $HD_p$ , MASD and ASSD because the overlap produces zero distances, therefore skewing the distance distribution towards lower values and reducing the sensitivity to boundary errors. Not surprisingly, nine out of the 11 open-source tools utilize boundary-based calculations, yet with considerably different boundary extraction methods (Fig. 2). But what exactly constitutes the boundary? In 2D, pixels are represented by rectangles, and the boundary between foreground and background pixels is logically located at their interface. While this is straightforward for straight, it becomes more complex for curved boundaries, where diagonals often represent the most natural transition. However, on discretized image grids, where boundary accuracy is constrained by the pixel size, *zig-zag* lines are often the only alternative (reducing the pixel size would improve boundary precision but impractically increase computational complexity [12]). Given these constraints, the most accurate boundary extraction method is employed by GoogleDeepMind and `pymia`, which shift the image grid by half a pixel/voxel size and therefore position the boundary precisely between the foreground and background, while other open-source tools use pixel/voxel centers that are essentially positioned within the foreground. Conversely, representing segmentations in the mesh space offers several advantages over its grid-based counterpart. First, discretization is directly controlled by *meshing*, resulting in a more accurate and continuous representation of the segmentation mask. Second, the boundary is inherently defined by the mesh contour/surface, eliminating the need for proprietary boundary extraction methods. Third, query point distances against an explicitly defined contour/surface yield more accurate calculations than grid-based methods that typically use the point-to-point Euclidean distance transform. Nevertheless, certain meshing-related considerations still exist, such as the choice of the meshing algorithm (Fig. A2 and Table A4).

Besides variations in boundary extraction, fundamental conceptual differences were observed across the open-source tools, which considerably impact metrics computation. We argue that the point-based definitions (`PointDef`, Fig. 3) are flawed due to their inherent assumption that query points are uniformly distributed across the boundary, which holds only for straight but not for curved boundaries (Fig. 2), and is even harder to justify for anisotropic grids. Among the 11 open-source tools, only GoogleDeepMind (and `pymia` that adopts its code) adjust for the non-uniformly distributed query points by approximating *marching cubes* on image grids. Empirically, this effect is particularly evident for anisotropic grids, where tools relying on the point-based definition perform significantly worse for HD,  $HD_p$ , MASD and ASSD when compared to GoogleDeepMind. However, because *marching cubes* provide only an approximation of the boundary, this approach performs well for HD,  $HD_p$ , MASD and ASSD, but we empirically observe that it introduces errors for NSD and BIoU that are more sensitive to boundary inaccuracies. In fact, all grid-based calculations are prone to discretization effects, leading to *quantized distances* – a finite set of distinct values determined by the pixel/voxel size and the arrangement of query points on the grid [12]. These effects become particularly pronounced when the pixel/voxel size and the parameter  $\tau$  of NSD and BIoU are of comparable magnitude. We hypothesize that *quantized distances* combined with *marching cubes* explain why GoogleDeepMind, despite being designed specifically for NSD, underperforms in comparison to MeshMetrics. Interestingly, other tools exhibit significant variations, but with a lower mean error, which we attribute to the circumstantial compounding effects of the employed boundary extraction methods and mathematical definitions. These considerations underscore the advantages of mesh-based computations, where distance calculations are implicit and not subjected to the limitations imposed by quantization.

The results presented in Fig. 4 and Table A1 revealed that for HD, the mean deviations are close to zero across all tools except for `MISeval` (Fig. 3), which highlights the general agreement on its mathematical definition supported by mostly non-significant statistical comparisons (Fig. A4). For  $HD_{95}$ , the results are more scattered due to larger differences in its mathematical definition. Particularly for large and tubular OARs (Table A2), `Plastimatch` produced the greatest outliers of up to  $-115$  mm due to the averaging of the directed percentile calculations rather than taking the maximum of both directed percentiles, which generates over-optimistic results. Similarly, over-optimistic performance is observed for `MedPy` and `seg-metrics`, both computing the percentile on the union of both distance sets (Fig. 3) that generally produces smaller metric values when coupled with their boundary extraction methods. Although `EvaluateSegmentation` applies the same calculation, it uses a different boundary extraction method that shifts the distribution toward higher distances and results in an over-pessimistic performance. While MONAI and `Metrics Reloaded` appear as the most accurate for isotropic grids, they exhibit several outliers and perform worse for the anisotropic grid. Notably, GoogleDeepMind is not only very close to these tools in terms of mean deviation for isotropic grids but also exhibits a greater precision, and outperforms in both accuracy and precision all other tools for the anisotropic grid. These findings align well with our conceptual analysis, as tools relying on the point-based definition (i.e. assume a uniform distribution of query points) performed significantly worse than GoogleDeepMind and `pymia`, which account for boundary element sizes (Fig. A1). Interestingly, low deviations in mean differences are observed for MASD and ASSD across all open-source tools, because averaging over large sets

of distances is statistically more stable and tends to conceal the variations in metrics implementation. However, it is crucial to also consider the range (min | max) of deviations, which further emphasize the need for unified mathematical definitions. For example, the comparison of `Google DeepMind` and `Metrics Reloaded` clearly demonstrates that the former is more consistent. Particularly for ASSD, these discrepancies are even more pronounced for the anisotropic grid.

Although supported by four open-source tools, only two distinct calculations are employed for NSD: a point-based by `Metrics Reloaded`/MONAI, and a mesh-based by `Google DeepMind`/pymia, with identical metric scores within pairs due to the same boundary extraction method. However, concerning outliers ranging from  $-16.1$  to  $34.8\%$ pt (Table A2) are consistently observed across OAR categories for both calculations, causing statistically significant differences against `MeshMetrics` and among the tools (Figure A4). As `Google DeepMind`, `Metrics Reloaded` and MONAI are deemed popular according to their GitHub stars ranking, questions are raised about the accuracy of existing studies applying these tools. For `Metrics Reloaded` and MONAI, the outliers can partly be attributed to not accounting for boundary element sizes, leading to an unjustified assumption of uniformly distributed query points. Surprisingly, even `Google DeepMind`, the original NSD implementation, shows signs of inaccuracy and imprecision, probably due to *quantized distances* coupled with the choice of  $\tau$ . As `MeshMetrics` uses implicit distance calculations, it is considerably less susceptible to quantization. These empirical findings highlight that, among all distance-based metrics, NSD is the most sensitive to distance and boundary calculations. As BIoU is a recently proposed metric, it is currently implemented only by `Metrics Reloaded`, which provides valid results only for the isotropic grid of unit size due to a flaw in its code, but still with significantly large deviations from `MeshMetrics` that range from  $-15.5$  to  $35.5\%$ pt and can be, similarly as for NSD, attributed to *quantized distances* coupled with the choice of  $\tau$ . We therefore suggest exercising caution when interpreting NSD and BIoU.

Statistical testing (Figure A4) reveals that all open-source tools exhibit significant differences against `MeshMetrics`, except `MedPy` and MONAI for MASD on the anisotropic grid. Perhaps even more surprising and concerning are the significant differences among the open-source tools, suggesting that even an objectively inferior segmentation may achieve superior metric scores simply due to utilizing a particular tool. For edge case handling (Table A3), we can conclude that it is critical that the tools provide clear and informative outputs, especially for users who are unaware of their functioning. Mishandling can lead to over-optimistic results, especially if edge cases are ignored or are unjustifiably assigned the best possible metric score. Although accurate measurement should remain the top priority, computational efficiency is a practical consideration when selecting an open-source tool. We observed considerable differences in median execution times across all open-source tools (Fig. A5), with `Google DeepMind` and MONAI being the most, and `MISEval`, `MedPy` and `Metrics Reloaded` the least time-efficient tools. With a median execution time of under 1 second per case, `MeshMetrics` ranks as the third most efficient tool, outperforming the majority of the 11 open-source tools. In addition, our analysis revealed several implementation flaws in the code of some open-source tools. `EvaluateSegmentation` employs optimization strategies [40] for HD that are incorrectly applied to  $HD_p$  and MASD, leading to skewed distance distributions that produce non-deterministic results, `MISEval` ignores the pixel/voxel size when calculating distances between query points, therefore performing relatively accurately only for the isotropic grid of unit size, and `Metrics Reloaded` exhibits a similar issue for BIoU.

In conclusion, we would first like to acknowledge the authors of the 11 open-source tools [1, 7, 8, 11–18] for their valuable contributions. The outcomes of our study should not be regarded as criticism, but rather as a constructive step towards proper metrics implementation and usage. Based on our detailed conceptual and quantitative analyses, we propose the following recommendations for distance-based metrics computation:

- Consult metrics selection guidelines, such as *Metrics Reloaded* [1], to identify representative metrics for the specific application.
- Ensure reproducibility by reporting the name and version of the open-source tool, as the choice of the tool can significantly impact the obtained results and their interpretation.
- Be mindful of edge case handling by not relying solely on open-source tools, but by implementing additional external conditioning.
- Pay attention to the correct usage of units of measurement and pixel/voxel sizes.
- Use `MeshMetrics` for highly accurate reference measurements. If not feasible, use `Google DeepMind` for HD,  $HD_p$ , MASD and ASSD due to its superior performance on both isotropic and anisotropic grids in comparison to other open-source tools, and exercise caution for NSD and BIoU due to implementation discrepancies.

We therefore hope that *Metrics Revolutions* with its groundbreaking insights will raise community awareness and understanding of the computational principles behind the distance-based metrics, and stimulate community members towards a more careful interpretation of segmentation results for both existing and future studies. As our findings suggest, studies that evaluated segmentation by using the 11 open-source tools may need to be revisited for implementation errors, and we eagerly contribute to this effort by offering `MeshMetrics` as a reference for the implementation of metrics for biomedical image segmentation.

## Acknowledgements

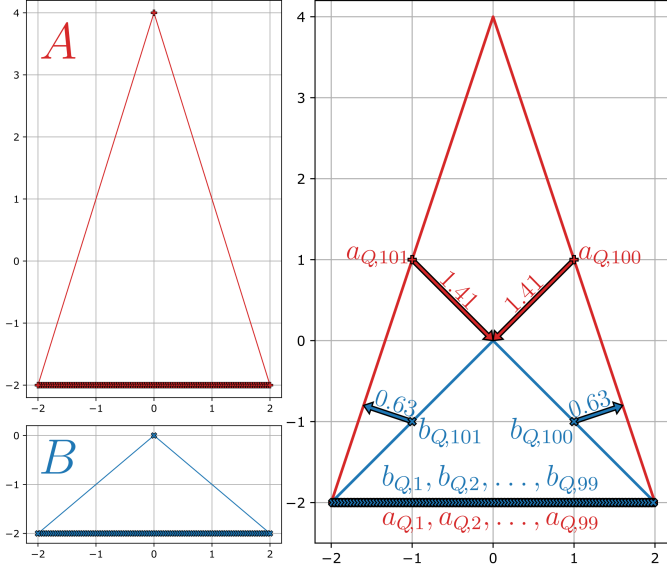
This study was supported by the Slovenian Research and Innovation Agency (ARIS) under projects No. J2-1732, J2-4453, J2-50067 and P2-0232, and by the European Union Horizon project ARTILLERY under grant agreement No. 101080983.

## References

1. Maier-Hein, L., Reinke, A., Godau, P., *et al.*: Metrics reloaded: Recommendations for image analysis validation. *Nat. Methods* **21**, 195–212 (2024) <https://doi.org/10.1038/s41592-023-02151-z>
2. Margolin, R., Zelnik-Manor, L., Tal, A.: How to evaluate foreground maps. In: *IEEE Conference on Computer Vision and Pattern Recognition - CVPR 2014*, pp. 248–255 (2014). <https://doi.org/10.1109/CVPR.2014.39>
3. Roß, T., Bruno, P., Reinke, A., *et al.*: Beyond rankings: Learning (more) from algorithm validation. *Med. Image Anal.* **86**, 102765 (2023) <https://doi.org/10.1016/j.media.2023.102765>
4. van den Oever, L.B., van Veldhuizen, W.A., Cornelissen, L.J., *et al.*: Qualitative evaluation of common quantitative metrics for clinical acceptance of automatic segmentation: a case study on heart contouring from CT images by deep learning algorithms. *J. Digit. Imaging* **35**, 240–247 (2022) <https://doi.org/10.1007/s10278-021-00573-9>
5. Antonelli, M., Reinke, A., Bakas, S., *et al.*: The Medical Segmentation Decathlon. *Nat. Commun.* **13**, 4128 (2022) <https://doi.org/10.1038/s41467-022-30695-9>
6. Ma, J., He, Y., Li, F., Han, L., You, C., Wang, B.: Segment anything in medical images. *Nat. Commun.* **15**, 654 (2024) <https://doi.org/10.1038/s41467-024-44824-z>
7. Taha, A.A., Hanbury, A.: Metrics for evaluating 3D medical image segmentation: analysis, selection, and tool. *BMC Med. Imaging* **15**, 29 (2015) <https://doi.org/10.1186/s12880-015-0068-x>
8. Müller, D., Soto-Rey, I., Kramer, F.: Towards a guideline for evaluation metrics in medical image segmentation. *BMC Res. Notes* **15**, 210 (2022) <https://doi.org/10.1186/s13104-022-06096-y>
9. Reinke, A., Tizabi, M.D., Baumgartner, M., *et al.*: Understanding metric-related pitfalls in image analysis validation. *Nat. Methods* **21**, 182–194 (2024) <https://doi.org/10.1038/s41592-023-02150-0>
10. Maier-Hein, L., Eisenmann, M., Reinke, A., *et al.*: Why rankings of biomedical image analysis competitions should be interpreted with care. *Nat. Commun.* **9**, 5217 (2018) <https://doi.org/10.1038/s41467-018-07619-7>
11. Commowick, O., Istace, A., Kain, M., *et al.*: Objective evaluation of multiple sclerosis lesion segmentation using a data management and processing infrastructure. *Sci. Rep.* **8**, 13650 (2018) <https://doi.org/10.1038/s41598-018-31911-7>
12. Nikolov, S., Blackwell, S., Zverovitch, A., *et al.*: Clinically applicable segmentation of head and neck anatomy for radiotherapy: deep learning algorithm development and validation study. *J. Med. Internet Res.* **23**, 26151 (2021) <https://doi.org/10.2196/26151>
13. Maier, O., Rothberg, A., Raamana, P.R., *et al.*: loli/medpy: MedPy 0.4.0. Zenodo (2019). <https://doi.org/10.5281/zenodo.2565940>
14. Cardoso, M.J., Li, W., Brown, R., *et al.*: MONAI: An open-source framework for deep learning in healthcare. *arXiv:2211.02701* (2022) <https://doi.org/10.48550/arXiv.2211.02701>
15. Zaffino, P., Raudaschl, P., Fritscher, K., Sharp, G.C., Spadea, M.F.: Technical Note: Plastimatch mabs, an open source tool for automatic image segmentation. *Med. Phys.* **43**, 5155 (2016) <https://doi.org/10.1118/1.4961121>
16. Jungo, A., Scheidegger, O., Reyes, M., Balsiger, F.: pymia: A Python package for data handling and evaluation in deep learning-based medical image analysis. *Comput. Methods Programs Biomed.* **198**, 105796 (2021) <https://doi.org/10.1016/j.cmpb.2020.105796>
17. Jia, J., Staring, M., Stoel, B.C.: seg-metrics: A Python package to compute segmentation metrics. *medRxiv* (2024) <https://doi.org/10.1101/2024.02.22.24303215>
18. Lowekamp, B., Chen, D., Ibanez, L., Blezek, D.: The design of SimpleITK. *Front. Neuroinform.* **7** (2013) <https://doi.org/10.3389/fninf.2013.00045>
19. Hausdorff, F.: *Grundzüge der Mengenlehre* [Basics of Set Theory]. Leipzig Viet, Leipzig, Germany (1914). <https://archive.org/details/grundzgedermen00hausuoft/>
20. Huttenlocher, D.P., Klanderman, G.A., Rucklidge, W.J.: Comparing images using the Hausdorff distance. *IEEE Trans. Pattern Anal. Mach. Intell.* **15**, 850–863 (1993) <https://doi.org/10.1109/34.232073>
21. Sluimer, I., Prokop, M., van Ginneken, B.: Toward automated segmentation of the pathological lung in CT. *IEEE Trans. Med. Imaging* **24**, 1025–1038 (2005) <https://doi.org/10.1109/TMI.2005.851757>
22. Lamecker, H., Lange, T., Seebass, M.: Segmentation of the liver using a 3D statistical shape model. *ZIB-Report* **04-09** (2004)
23. Cheng, B., Girshick, R.B., Dollár, P., Berg, A.C., Kirillov, A.: Boundary IoU: Improving object-centric image segmentation evaluation. In: *IEEE/CVF Conference on Computer Vision and Pattern Recognition - CVPR 2021*, pp. 15329–15337 (2021). <https://doi.org/10.1109/CVPR46437.2021.01508>
24. Alt, H., Guibas, L.J.: Discrete geometric shapes: matching, interpolation, and approximation. In: *Handbook of Computational Geometry*, pp. 121–153. Elsevier, Amsterdam, The Netherlands (2000). Chap. 3. <https://doi.org/10.1016/B978-0-444-82537-7.X5000-1>

25. Drukker, K., Sahiner, B., Hu, T., *et al.*: MIDRC-MetricTree: A decision tree-based tool for recommending performance metrics in artificial intelligence-assisted medical image analysis. *J. Med. Imaging* **11**, 024504 (2024) <https://doi.org/10.1117/1.JMI.11.2.024504>
26. Maier-Hein, L., Reinke, A., Christodoulou, E., *et al.*: Metrics reloaded: Pitfalls and recommendations for image analysis validation. arXiv:2206.01653v1 (2022) <https://doi.org/10.48550/arXiv.2206.01653>
27. Brown, B.B.: *Delphi Process: A Methodology Used for the Elicitation of Opinions of Experts*. RAND Corporation, Santa Monica, CA (1968)
28. Fedorov, A., Beichel, R., Kalpathy-Cramer, J., *et al.*: 3D Slicer as an image computing platform for the Quantitative Imaging Network. *Magn. Reson. Imaging* **30**, 1323–1341 (2012) <https://doi.org/10.1016/j.mri.2012.05.001>
29. Schroeder, W., Maynard, R., Geveci, B.: Flying edges: A high-performance scalable isocontouring algorithm. In: 5th Symposium on Large Data Analysis and Visualization - LDAV 2015, pp. 33–40 (2015). <https://doi.org/10.1109/LDAV.2015.7348069>
30. Grothausmann, R.: Providing values of adjacent voxel with vtkDiscreteMarchingCubes. *VTK J.* (2016) <https://doi.org/10.54294/2aeqx3>
31. Duprez, M., Bordas, S.P.A., Bucki, M., *et al.*: Quantifying discretization errors for soft tissue simulation in computer assisted surgery: a preliminary study. *Appl. Math. Model.* **77**, 709–723 (2020) <https://doi.org/10.1016/j.apm.2019.07.055>
32. Podobnik, G., Strojjan, P., Peterlin, P., Ibragimov, B., Vrtovec, T.: HaN-Seg: The head and neck organ-at-risk CT and MR segmentation dataset. *Med. Phys.* **50**, 1917–1927 (2023) <https://doi.org/10.1002/mp.16197>
33. Podobnik, G., Strojjan, P., Peterlin, P., Ibragimov, B., Vrtovec, T.: Multimodal CT and MR segmentation of head and neck organs-at-risk. In: 26th International Conference on Medical Image Computing and Computer-Assisted Intervention - MICCAI 2023. *Lecture Notes in Computer Science*, vol. 14223, pp. 745–755. Springer, Vancouver, Canada (2023). [https://doi.org/10.1007/978-3-031-43901-8\\_71](https://doi.org/10.1007/978-3-031-43901-8_71)
34. Podobnik, G., Ibragimov, B., Strojjan, P., Peterlin, P., Vrtovec, T.: vOARiability: Interobserver and intermodality variability analysis in OAR contouring from head and neck CT and MR images. *Med. Phys.* **51**, 2175–2186 (2024) <https://doi.org/10.1002/mp.16924>
35. Podobnik, G., Ibragimov, B., Tappeiner, E., *et al.*: HaN-Seg: The head and neck organ-at-risk CT and MR segmentation challenge. *Radiother. Oncol.* **198**, 110410 (2024) <https://doi.org/10.1016/j.radonc.2024>
36. Isensee, F., Jaeger, P.F., Kohl, S.A.A., Petersen, J., Maier-Hein, K.H.: nnU-Net: A self-configuring method for deep learning-based biomedical image segmentation. *Nat. Methods* **18**, 203–211 (2021) <https://doi.org/10.1038/s41592-020-01008-z>
37. Vrtovec, T., Močnik, D., Strojjan, P., Pernuš, F., Ibragimov, I.: Auto-segmentation of organs at risk for head and neck radiotherapy planning: from atlas-based to deep learning methods. *Med. Phys.* **47**, 929–950 (2020) <https://doi.org/10.1002/mp.14320>
38. Ye, X., Guo, D., Ge, J., *et al.*: Comprehensive and clinically accurate head and neck cancer organs-at-risk delineation on a multi-institutional study. *Nat. Commun.* **13**, 6137 (2022) <https://doi.org/10.1038/s41467-022-33178-z>
39. Aydin, O.U., Taha, A.A., Hilbert, A., *et al.*: On the usage of average Hausdorff distance for segmentation performance assessment: hidden error when used for ranking. *Eur. Radiol. Exp.* **5**, 4 (2021) <https://doi.org/10.1186/s41747-020-00200-2>
40. Taha, A.A., Hanbury, A.: An efficient algorithm for calculating the exact Hausdorff distance. *IEEE Trans. Pattern Anal. Mach. Intell.* **37**, 2153–2163 (2015) <https://doi.org/10.1109/TPAMI.2015.2408351>
41. Nielson, G.M., Hamann, B.: The asymptotic decider: resolving the ambiguity in marching cubes. In: *Proceeding Visualization '91*, pp. 83–91 (1991). <https://doi.org/10.1109/VISUAL.1991.175782>
42. Gibson, S.F.F.: Constrained elastic surface nets: generating smooth surfaces from binary segmented data. In: 1st International Conference on Medical Image Computing and Computer-Assisted Intervention - MICCAI 1998. *Lecture Notes in Computer Science*, vol. 1496, pp. 888–898. Springer, Cambridge, MA, USA (1998). <https://doi.org/10.1007/BFb0056277>

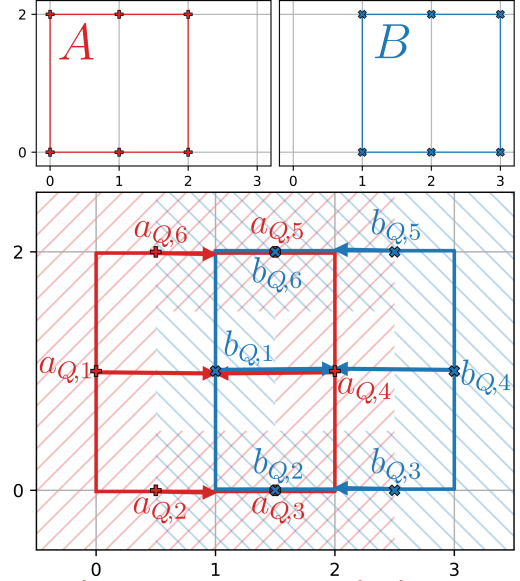




$$\begin{aligned}
 D_{AB} &= \{d_{a_{Q,1}}, d_{a_{Q,2}}, \dots, d_{a_{Q,99}}, d_{a_{Q,100}}, d_{a_{Q,101}}\} = \{0, 0, \dots, 0, 1.41, 1.41\} \\
 D_{BA} &= \{d_{b_{Q,1}}, d_{b_{Q,2}}, \dots, d_{b_{Q,99}}, d_{b_{Q,100}}, d_{b_{Q,101}}\} = \{0, 0, \dots, 0, 0.63, 0.63\} \\
 S_{AB} &= \{s_{a_{Q,1}}, s_{a_{Q,2}}, \dots, s_{a_{Q,99}}, s_{a_{Q,100}}, s_{a_{Q,101}}\} = \{0.04, 0.04, \dots, 0.04, 6.32, 6.32\} \\
 S_{BA} &= \{s_{b_{Q,1}}, s_{b_{Q,2}}, \dots, s_{b_{Q,99}}, s_{b_{Q,100}}, s_{b_{Q,101}}\} = \{0.04, 0.04, \dots, 0.04, 2.83, 2.83\}
 \end{aligned}$$

PointDef	$[D_{AB}]_p = 0.00$	$[D_{BA}]_p = 0.00$	$HD_{95} = 0.00$	MASD = 0.02	ASSD = 0.02
MeshMetrics	$D_{AB, m_{95}} = 1.41$	$D_{BA, m_{95}} = 0.63$	$HD_{95} = 1.41$	MASD = 0.72	ASSD = 0.82

(a) Two isosceles triangles on an isotropic grid, with a shared base but different apex points.

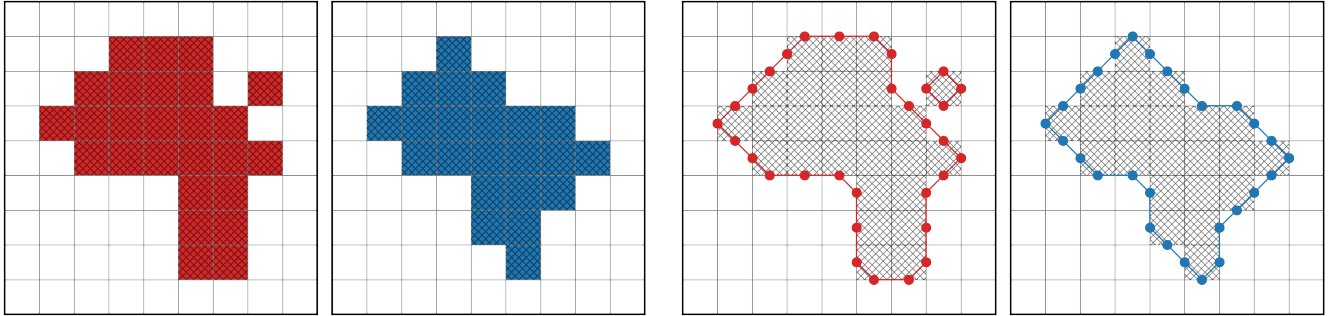


$$\begin{aligned}
 D_{AB} &= \{d_{a_{Q,3}}, d_{a_{Q,5}}, d_{a_{Q,2}}, d_{a_{Q,6}}, d_{a_{Q,1}}, d_{a_{Q,4}}\} = \{0, 0, 0.5, 0.5, 1, 1\} \\
 D_{BA} &= \{d_{b_{Q,2}}, d_{b_{Q,6}}, d_{b_{Q,3}}, d_{b_{Q,5}}, d_{b_{Q,1}}, d_{b_{Q,4}}\} = \{0, 0, 0.5, 0.5, 1, 1\} \\
 S_{AB} &= \{s_{a_{Q,3}}, s_{a_{Q,5}}, s_{a_{Q,2}}, s_{a_{Q,6}}, s_{a_{Q,1}}, s_{a_{Q,4}}\} = \{1, 1, 1, 1, 2, 2\} \\
 S_{BA} &= \{s_{b_{Q,3}}, s_{b_{Q,5}}, s_{b_{Q,2}}, s_{b_{Q,6}}, s_{b_{Q,1}}, s_{b_{Q,4}}\} = \{1, 1, 1, 1, 2, 2\}
 \end{aligned}$$

PointDef	$NSD_{r=0.5} = 66.7\%$	$BIoU_{r=0.5} = 50\%$
MeshMetrics	$NSD_{r=0.5} = 50\%$	$BIoU_{r=0.5} = 20\%$

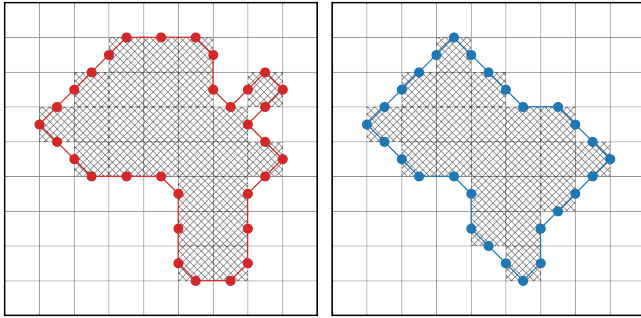
(b) Two square polygons on an anisotropic grid, with one shifted by 1 unit along the horizontal axis.

**Fig. A1.** Two conceptual examples that help in understanding the importance of the boundary element size for distance-based metrics computation. (a) Let  $A_P$  and  $B_P$  represent the point sets of two closed polygons forming two isosceles triangles on an isotropic grid, where 100 points are uniformly placed at each triangle base and one point at each triangle tip. The only difference between the two triangles is that the tip of triangle  $B$  is located 4 units lower than the tip of  $A$ , which is reflected in their relatively small overlap ( $DSC = 0.5$ ). Each triangle therefore consists of 101 boundary elements represented by line segments, with query points located at their midpoints, i.e. 99 at the base and two at the sides. The distances from  $A$  to  $B$  are zero for the 99 base query points because of the perfect overlap, and 1.41 for the two side query points. Similarly, the distances from  $B$  to  $A$  are zero for the 99 base query points, and 0.63 for the two side query points. If we calculate  $HD_{95}$  using the established mathematical definition, we take the 96-th out of 101 elements in the set of ascendingly ordered distances, which correspond to  $[D_{AB}]_{95} = 0$  and  $[D_{BA}]_{95} = 0$ , and result in  $HD_{95} = 0$ . On the other hand, if we take into account the length of the line segments, we yield  $[D_{AB}]_{95} = 1.41$  and  $[D_{BA}]_{95} = 0.63$  that result in  $HD_{95} = 1.41$ , which better reflects the actual differences between the two triangles. Because the query points are not uniformly distributed across the boundary, which is often the case in real-world applications, this experiment shows that the computation of  $HD_p$  that is based solely on distances may result in misleading conclusions. (b) Let  $A_P$  and  $B_P$  represent the point sets of two closed polygons forming two squares on an anisotropic grid, with the only difference that one square is shifted by 1 unit along the horizontal axis so that both squares overlap by half. Like for the previous example, the query points are positioned at the midpoints of line segments, and corresponding distances and boundary element sizes are calculated. If the resulting sets of distances are used to calculate  $NSD$  and  $BIoU$ , we can observe that the **PointDef** definition fails to account for the anisotropic grid and produces overoptimistic scores of  $NSD = 66.7\%$  and  $BIoU = 50\%$ , as it does not weigh the contribution of each distance by the corresponding boundary element size. Conversely, the **MeshMetrics** definition accounts for the anisotropic effect, yielding correct scores of  $NSD = 50\%$  and  $BIoU = 20\%$ . In relation to both conceptual examples, it has to be noted that in practice the number of query points is considerably larger, and that differences in metric scores depend also on the geometry of the two segmentation masks.

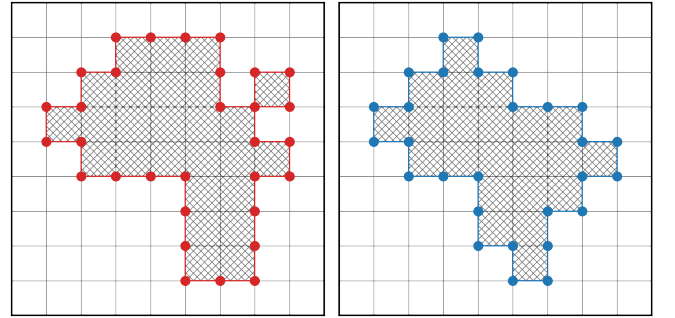


(a) Example segmentation masks  $A$  and  $B$ .

(b) *Marching squares* in 2D, analogous to *marching cubes* in 3D.



(c) *Discrete flying edges* in 2D, analogous to *discrete marching cubes* in 3D.

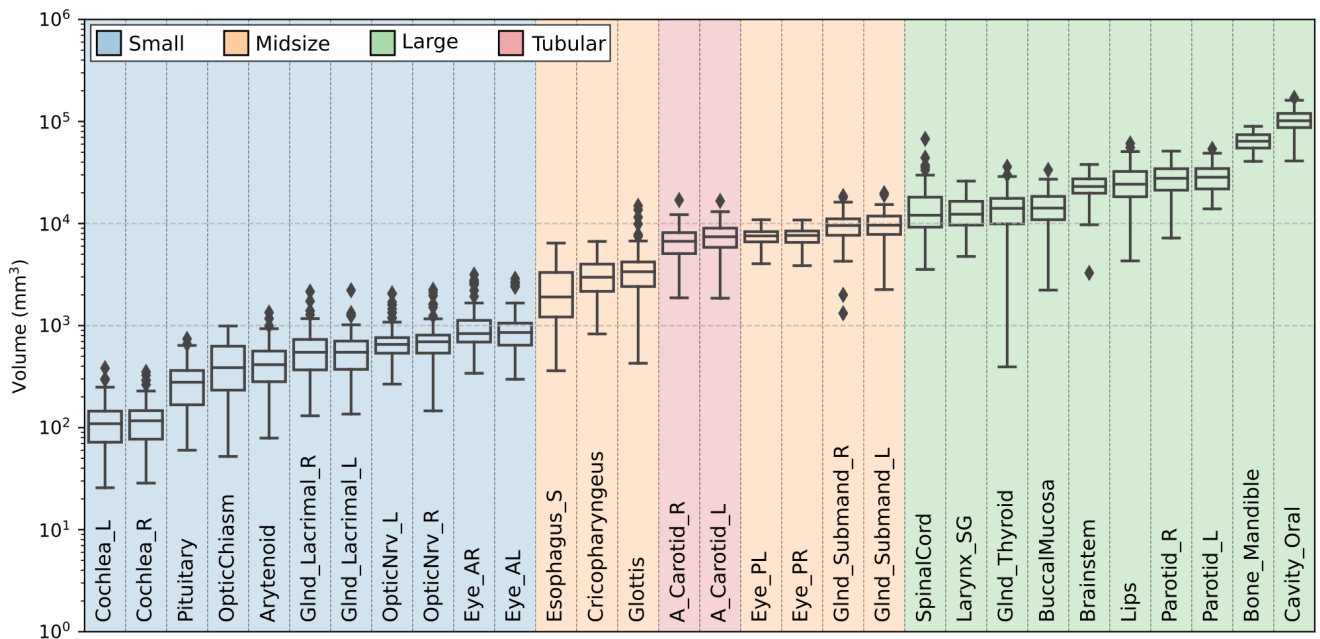


(d) *Surface nets* in 2D, analogous to *surface nets* in 3D.

**Fig. A2.** Overview of methods for the conversion of binary segmentation masks to meshes, often referred to as *isosurface extraction* or simply *meshing*. All methods are demonstrated using 2D binary segmentation masks with an isosurface value set to 0.5 where applied, and their analogous methods in 3D are also noted. (a) The *marching squares* / *marching cubes* algorithm is the traditional and widely adopted meshing algorithm that produces smooth results. (b) The *discrete flying edges* / *discrete marching cubes* algorithm [29, 30] builds upon the traditional algorithm but is non-parametric (i.e. does not require an isosurface value) and handles ambiguous cases more conveniently for most image segmentation tasks [41], such as in the shown example, where a single instead of two connected components is produced. As a result, this algorithm is used by our reference implementation **MeshMetrics**. (c) The *surface nets* algorithm [42] closely resembles the boundary extraction method employed by **Google DeepMind** and **pymia**. However, the resulting *zig-zag* boundaries introduce unnatural and unrealistic artifacts. The results of a detailed quantitative analysis are for all meshing algorithms presented in Table A4.

**Table A1.** The differences ( $\Delta$ ) in the distance-based metrics, as obtained by each open-source tool against the reference implementation *MeshMetrics* on 1,561 pairs of OAR segmentation masks, reported for two isotropic and one anisotropic voxel size as the range min|max and mean  $\pm$  standard deviation (SD).

Open-source tool	Voxel size					
	(1.0, 1.0, 1.0) mm		(2.0, 2.0, 2.0) mm		(0.5, 0.5, 2.0) mm	
<b><math>\Delta</math> HD (mm)</b>	min max	Mean $\pm$ SD	min max	Mean $\pm$ SD	min max	Mean $\pm$ SD
Anima	-6.30 0.32	<b>0.02<math>\pm</math>0.25</b>	-6.28 0.79	0.11 $\pm$ 0.29	-6.45 1.02	<b>0.03<math>\pm</math>0.27</b>
EvaluateSegmentation	-6.30 0.32	<b>0.02<math>\pm</math>0.25</b>	-6.28 0.79	0.11 $\pm$ 0.29	-6.45 1.02	<b>0.03<math>\pm</math>0.27</b>
Google DeepMind	<b>-0.56 0.27</b>	0.03 $\pm$ 0.09	-1.29  <b>0.67</b>	<b>0.09<math>\pm</math>0.19</b>	-0.83  <b>0.28</b>	<b>0.03<math>\pm</math>0.08</b>
MedPy	-0.65 0.32	0.05 $\pm$ 0.06	<b>-1.19 0.79</b>	0.12 $\pm$ 0.15	<b>-0.50 1.02</b>	0.05 $\pm$ 0.06
Metrics Reloaded	-0.65 0.32	0.05 $\pm$ 0.06	<b>-1.19 0.79</b>	0.12 $\pm$ 0.15	<b>-0.50 1.02</b>	0.05 $\pm$ 0.06
MISeval	-6.30 0.32	<b>0.02<math>\pm</math>0.25</b>	-124 -0.68	-5.01 $\pm$ 6.63	-123 43.0	2.92 $\pm$ 7.09
MONAI	-0.65 0.32	0.05 $\pm$ 0.06	<b>-1.19 0.79</b>	0.12 $\pm$ 0.15	<b>-0.50 1.02</b>	0.05 $\pm$ 0.06
Plastimatch	-0.65 0.32	0.05 $\pm$ 0.06	<b>-1.19 0.79</b>	0.13 $\pm$ 0.15	<b>-0.50 1.02</b>	0.05 $\pm$ 0.06
pymia	<b>-0.56 0.27</b>	0.03 $\pm$ 0.09	-1.29  <b>0.67</b>	<b>0.09<math>\pm</math>0.19</b>	-0.83  <b>0.28</b>	<b>0.03<math>\pm</math>0.08</b>
seg-metrics	-0.94 9.58	0.07 $\pm$ 0.35	-1.25 0.79	0.12 $\pm$ 0.15	-0.79 1.02	0.05 $\pm$ 0.07
SimpleITK	-6.30 0.32	<b>0.02<math>\pm</math>0.25</b>	-6.28 0.79	0.11 $\pm$ 0.29	-6.45 1.02	<b>0.03<math>\pm</math>0.27</b>
<b><math>\Delta</math> HD<sub>p</sub> (mm)</b>	min max	Mean $\pm$ SD	min max	Mean $\pm$ SD	min max	Mean $\pm$ SD
EvaluateSegmentation	<b>-0.13 16.1</b>	2.80 $\pm$ 2.69	<b>-0.39 17.4</b>	2.66 $\pm$ 2.68	<b>-0.10 16.2</b>	2.89 $\pm$ 2.67
Google DeepMind	-0.72  <b>0.42</b>	-0.16 $\pm$ 0.17	-1.63  <b>0.83</b>	-0.21 $\pm$ 0.39	-0.70  <b>0.83</b>	<b>-0.08<math>\pm</math>0.18</b>
MedPy	-17.6 0.58	-0.83 $\pm$ 1.63	-18.6 1.23	-0.71 $\pm$ 1.74	-16.5 2.24	-0.51 $\pm$ 1.33
Metrics Reloaded	-4.67 1.59	<b>0.06<math>\pm</math>0.25</b>	-7.63 1.80	<b>0.15<math>\pm</math>0.47</b>	-4.77 7.60	0.34 $\pm$ 0.82
MONAI	-4.67 1.59	<b>0.06<math>\pm</math>0.25</b>	-7.63 1.80	<b>0.15<math>\pm</math>0.47</b>	-4.77 7.60	0.34 $\pm$ 0.82
Plastimatch	-115 0.58	-1.97 $\pm$ 5.75	-115  <b>0.83</b>	-1.86 $\pm$ 5.75	-111 1.83	-1.76 $\pm$ 5.56
pymia	-0.72  <b>0.42</b>	-0.16 $\pm$ 0.17	-1.63  <b>0.83</b>	-0.21 $\pm$ 0.39	-0.70  <b>0.83</b>	<b>-0.08<math>\pm</math>0.18</b>
seg-metrics	-19.4 0.44	-1.22 $\pm$ 1.86	-18.6  <b>0.83</b>	-0.99 $\pm$ 1.90	-17.1 1.03	-0.81 $\pm$ 1.56
<b><math>\Delta</math> MASD (mm)</b>	min max	Mean $\pm$ SD	min max	Mean $\pm$ SD	min max	Mean $\pm$ SD
Anima	-0.46 37.9	0.59 $\pm$ 1.69	<b>-0.03 40.5</b>	0.72 $\pm$ 1.76	<b>-0.23 32.5</b>	0.70 $\pm$ 1.75
EvaluateSegmentation	-2.79 2.45	-0.57 $\pm$ 0.44	-2.50 2.36	-0.39 $\pm$ 0.49	-2.89 4.23	-0.52 $\pm$ 0.48
Google DeepMind	-0.39  <b>-0.03</b>	-0.15 $\pm$ 0.03	-0.79  <b>-0.04</b>	-0.28 $\pm$ 0.07	-0.25  <b>-0.02</b>	-0.15 $\pm$ 0.02
MedPy	-37.5 14.4	0.10 $\pm$ 1.79	-37.4 14.0	0.15 $\pm$ 1.80	-36.9 17.1	0.12 $\pm$ 1.89
Metrics Reloaded	<b>-0.36 0.83</b>	<b>0.07<math>\pm</math>0.07</b>	-1.30 1.57	<b>0.13<math>\pm</math>0.16</b>	-2.37 1.75	<b>0.09<math>\pm</math>0.28</b>
MONAI	-37.5 14.4	0.10 $\pm$ 1.79	-37.4 14.0	0.15 $\pm$ 1.80	-36.9 17.1	0.12 $\pm$ 1.89
Plastimatch	<b>-0.36 0.83</b>	<b>0.07<math>\pm</math>0.07</b>	-1.30 1.57	<b>0.13<math>\pm</math>0.17</b>	-2.37 1.75	<b>0.09<math>\pm</math>0.28</b>
pymia	-2.79 2.45	-0.57 $\pm$ 0.44	-2.50 2.36	-0.39 $\pm$ 0.49	-2.89 2.87	-0.55 $\pm$ 0.45
SimpleITK	-2.79 2.45	-0.57 $\pm$ 0.44	-2.50 2.36	-0.39 $\pm$ 0.49	-2.89 2.87	-0.55 $\pm$ 0.45
<b><math>\Delta</math> ASSD (mm)</b>	min max	Mean $\pm$ SD	min max	Mean $\pm$ SD	min max	Mean $\pm$ SD
Anima	-22.9 0.53	-1.33 $\pm$ 1.28	-22.7 1.96	-1.27 $\pm$ 1.25	-22.8 1.61	-1.22 $\pm$ 1.27
Google DeepMind	<b>-0.40 -0.03</b>	-0.15 $\pm$ 0.03	<b>-0.79 -0.04</b>	-0.29 $\pm$ 0.07	<b>-0.25 -0.02</b>	-0.15 $\pm$ 0.02
Metrics Reloaded	-0.60 1.60	<b>0.07<math>\pm</math>0.09</b>	-1.98 2.89	0.15 $\pm$ 0.19	-4.55 2.88	0.10 $\pm$ 0.34
MONAI	-0.60 1.60	<b>0.07<math>\pm</math>0.09</b>	-1.98 2.89	0.15 $\pm$ 0.19	-4.55 2.88	0.10 $\pm$ 0.34
seg-metrics	-1.91 0.62	-0.14 $\pm$ 0.16	-3.29 1.24	<b>-0.12<math>\pm</math>0.27</b>	-4.09 1.81	<b>-0.07<math>\pm</math>0.26</b>
<b><math>\Delta</math> NSD <math>\tau=2</math> mm (%pt)</b>	min max	Mean $\pm$ SD	min max	Mean $\pm$ SD	min max	Mean $\pm$ SD
Google DeepMind	<b>-0.01 16.4</b>	2.99 $\pm$ 2.06	<b>0.00 34.8</b>	6.30 $\pm$ 4.63	<b>-4.25 10.2</b>	1.82 $\pm$ 1.53
Metrics Reloaded	-9.05  <b>7.09</b>	<b>0.28<math>\pm</math>1.31</b>	-13.2  <b>14.6</b>	<b>1.70<math>\pm</math>2.82</b>	-16.1 12.5	<b>-1.69<math>\pm</math>3.48</b>
MONAI	-9.05  <b>7.09</b>	<b>0.28<math>\pm</math>1.31</b>	-13.2  <b>14.6</b>	<b>1.70<math>\pm</math>2.82</b>	-16.1 12.5	<b>-1.69<math>\pm</math>3.48</b>
pymia	<b>-0.01 16.4</b>	2.99 $\pm$ 2.06	<b>0.00 34.8</b>	6.30 $\pm$ 4.63	<b>-4.25 10.2</b>	1.82 $\pm$ 1.53
<b><math>\Delta</math> BioU <math>\tau=2</math> mm (%pt)</b>	min max	Mean $\pm$ SD	min max	Mean $\pm$ SD	min max	Mean $\pm$ SD
Metrics Reloaded	<b>-15.5 35.5</b>	<b>5.47<math>\pm</math>5.06</b>	<b>-14.4 38.3</b>	<b>18.4<math>\pm</math>9.94</b>	<b>-19.6 36.9</b>	<b>3.00<math>\pm</math>6.40</b>



**OAR labels** – A.Carotid.L: left carotid artery, A.Carotid.R: right carotid artery, Arytenoid: arytenoids, Bone.Mandible: mandible, Brainstem: brainstem, BuccalMucosa: buccal mucosa, Cavity.Oral: oral cavity, Cochlea.L: left cochlea, Cochlea.R: right cochlea, Cricopharyngeus: cricopharyngeal inlet, Esophagus.S: cervical esophagus, Eye.AL: anterior segment of the left eyeball, Eye.AR: anterior segment of the right eyeball, Eye.PL: posterior segment of the left eyeball, Eye.PR: posterior segment of the right eyeball, GlnD.Lacrimal.L: left lacrimal gland, GlnD.Lacrimal.R: right lacrimal gland, GlnD.Submand.L: left submandibular gland, GlnD.Submand.R: right submandibular gland, GlnD.Thyroid: thyroid gland, Glottis: glottic larynx, Larynx.SG: supraglottic larynx, Lips: lips, Musc.Constrict: pharyngeal constrictor muscles, OpticChiasm: optic chiasm, OpticNrv.L: left optic nerve, OpticNrv.R: right optic nerve, Parotid.L: left parotid gland, Parotid.R: right parotid gland, Pituitary: pituitary gland, SpinalCord: spinal cord.

**Fig. A3.** The complete collection of 30 OARs in the head and neck region of the *HaN-Seg* dataset [32, 34] that were used for distance-based metrics computation within our segmentation experiment on real-world data, with their volume  $V$  shown in the form of box-plots. According to their median volume  $\tilde{V}$ , OARs with  $\tilde{V} \leq 10^3 \text{ mm}^3$  were categorized as *small*, OARs with  $10^3 \text{ mm}^3 < \tilde{V} \leq 10^4 \text{ mm}^3$  were categorized as *midsize*, and OARs with  $\tilde{V} > 10^4 \text{ mm}^3$  were categorized as *large*. The left and right carotid arteries (A.Carotid.L and A.Carotid.R) were further categorized as *tubular*, as such vessel-like structures often exhibit anomalies for specific metric scores. The results of a detailed quantitative analysis of distance-based metrics computation are for different OAR categories presented in Table A2.

**Table A2.** The differences ( $\Delta$ ) in the distance-based metrics, as computed by each open-source tool against our reference implementation `MeshMetrics` on 1,561 pairs of OAR segmentation masks, aggregated across all voxel sizes but stratified according to the OAR category into small, midsize, large and tubular (cf. Fig. A3), and reported as the range min | max and mean  $\pm$  standard deviation (SD).

Open-source tool	OAR category							
	Small		Midsize		Large		Tubular	
$\Delta$ HD (mm)	min   max	Mean $\pm$ SD	min   max	Mean $\pm$ SD	min   max	Mean $\pm$ SD	min   max	Mean $\pm$ SD
Anima	<b>-0.36 0.67</b>	0.09 $\pm$ 0.09	-2.25  <b>0.64</b>	0.04 $\pm$ 0.20	-6.45  <b>0.66</b>	<b>0.02<math>\pm</math>0.42</b>	<b>-0.13 1.02</b>	0.09 $\pm$ 0.11
EvaluateSegmentation	<b>-0.36 0.67</b>	0.09 $\pm$ 0.09	-2.25  <b>0.64</b>	0.04 $\pm$ 0.20	-6.45  <b>0.66</b>	<b>0.02<math>\pm</math>0.42</b>	<b>-0.13 1.02</b>	0.09 $\pm$ 0.11
Google DeepMind	-0.55  <b>0.67</b>	<b>0.08<math>\pm</math>0.10</b>	-0.93  <b>0.64</b>	<b>0.03<math>\pm</math>0.15</b>	-1.29  <b>0.66</b>	0.04 $\pm$ 0.14	-0.83  <b>0.65</b>	<b>0.07<math>\pm</math>0.12</b>
MedPy	<b>-0.36 0.67</b>	0.09 $\pm$ 0.09	<b>-0.77 0.64</b>	0.07 $\pm$ 0.11	<b>-1.19 0.66</b>	0.06 $\pm$ 0.11	<b>-0.13 1.02</b>	0.09 $\pm$ 0.11
Metrics Reloaded	<b>-0.36 0.67</b>	0.09 $\pm$ 0.09	<b>-0.77 0.64</b>	0.07 $\pm$ 0.11	<b>-1.19 0.66</b>	0.06 $\pm$ 0.11	<b>-0.13 1.02</b>	0.09 $\pm$ 0.11
MISeval	-15.7 21.6	0.15 $\pm$ 3.58	-16.6 14.8	-0.75 $\pm$ 3.05	-124 43.0	-1.14 $\pm$ 9.46	-47.0 15.4	-2.26 $\pm$ 7.84
MONAI	<b>-0.36 0.67</b>	0.09 $\pm$ 0.09	<b>-0.77 0.64</b>	0.07 $\pm$ 0.11	<b>-1.19 0.66</b>	0.06 $\pm$ 0.11	<b>-0.13 1.02</b>	0.09 $\pm$ 0.11
Plastimatch	<b>-0.36 0.67</b>	0.09 $\pm$ 0.09	<b>-0.77 0.64</b>	0.07 $\pm$ 0.11	<b>-1.19 0.66</b>	0.06 $\pm$ 0.11	<b>-0.13 1.02</b>	0.09 $\pm$ 0.11
pymia	-0.55  <b>0.67</b>	<b>0.08<math>\pm</math>0.10</b>	-0.93  <b>0.64</b>	<b>0.03<math>\pm</math>0.15</b>	-1.29  <b>0.66</b>	0.04 $\pm$ 0.14	-0.83  <b>0.65</b>	<b>0.07<math>\pm</math>0.12</b>
seg-metrics	<b>-0.36 0.67</b>	0.09 $\pm$ 0.09	-0.89 2.27	0.07 $\pm$ 0.18	-1.25 9.58	0.08 $\pm$ 0.34	<b>-0.13 1.02</b>	0.09 $\pm$ 0.11
SimpleITK	<b>-0.36 0.67</b>	0.09 $\pm$ 0.09	-2.25  <b>0.64</b>	0.04 $\pm$ 0.20	-6.45  <b>0.66</b>	<b>0.02<math>\pm</math>0.42</b>	<b>-0.13 1.02</b>	0.09 $\pm$ 0.11
$\Delta$ HD <sub>p</sub> (mm)	min   max	Mean $\pm$ SD	min   max	Mean $\pm$ SD	min   max	Mean $\pm$ SD	min   max	Mean $\pm$ SD
EvaluateSegmentation	<b>-0.29 5.21</b>	1.01 $\pm$ 0.75	<b>-0.10 6.49</b>	1.65 $\pm$ 1.06	<b>-0.39 17.4</b>	4.61 $\pm$ 2.72	<b>0.46 15.2</b>	6.27 $\pm$ 3.23
Google DeepMind	-1.54  <b>0.83</b>	-0.13 $\pm$ 0.29	-0.87 0.83	<b>-0.09<math>\pm</math>0.26</b>	-1.18  <b>0.83</b>	<b>-0.20<math>\pm</math>0.25</b>	-1.63  <b>0.67</b>	<b>-0.19<math>\pm</math>0.29</b>
MedPy	-7.45 0.99	-0.28 $\pm$ 0.69	-3.73 0.83	-0.27 $\pm$ 0.53	-16.5 2.24	-1.08 $\pm$ 1.92	-18.6 1.52	-2.12 $\pm$ 3.07
Metrics Reloaded	-1.88 1.67	<b>0.11<math>\pm</math>0.30</b>	-0.80 3.18	0.17 $\pm$ 0.33	-4.77 7.60	0.22 $\pm$ 0.75	-7.63 4.22	0.32 $\pm$ 1.04
MONAI	-1.88 1.67	<b>0.11<math>\pm</math>0.30</b>	-0.80 3.18	0.17 $\pm$ 0.33	-4.77 7.60	0.22 $\pm$ 0.75	-7.63 4.22	0.32 $\pm$ 1.04
Plastimatch	-8.84  <b>0.83</b>	-1.07 $\pm$ 1.36	-14.0 1.02	-1.18 $\pm$ 1.90	-115 1.83	-2.83 $\pm$ 8.85	-42.9 1.42	-3.29 $\pm$ 6.73
pymia	-1.54  <b>0.83</b>	-0.13 $\pm$ 0.29	-0.87 0.83	<b>-0.09<math>\pm</math>0.26</b>	-1.18  <b>0.83</b>	<b>-0.20<math>\pm</math>0.25</b>	-1.63  <b>0.67</b>	<b>-0.19<math>\pm</math>0.29</b>
seg-metrics	-8.49  <b>0.83</b>	-0.41 $\pm$ 0.78	-4.37  <b>0.78</b>	-0.60 $\pm$ 0.76	-14.8 1.03	-1.53 $\pm$ 2.11	-19.4 0.81	-2.67 $\pm$ 3.46
$\Delta$ MASD (mm)	min   max	Mean $\pm$ SD	min   max	Mean $\pm$ SD	min   max	Mean $\pm$ SD	min   max	Mean $\pm$ SD
Anima	<b>-0.22 4.99</b>	0.52 $\pm$ 0.57	-0.46 5.73	0.51 $\pm$ 0.77	<b>-0.18 40.5</b>	0.90 $\pm$ 2.66	<b>-0.06 17.1</b>	0.83 $\pm$ 2.07
EvaluateSegmentation	-1.36 4.23	-0.17 $\pm$ 0.37	-1.78 0.85	-0.53 $\pm$ 0.27	-2.63 2.87	-0.83 $\pm$ 0.48	-2.89 1.12	-0.35 $\pm$ 0.35
Google DeepMind	-0.79  <b>-0.02</b>	-0.20 $\pm$ 0.09	-0.46  <b>-0.05</b>	-0.18 $\pm$ 0.06	-0.46  <b>-0.03</b>	-0.20 $\pm$ 0.07	-0.47  <b>-0.09</b>	-0.18 $\pm$ 0.06
MedPy	-2.69 4.99	0.20 $\pm$ 0.70	-4.75 5.45	<b>0.11<math>\pm</math>0.86</b>	-37.5 14.5	<b>-0.01<math>\pm</math>2.78</b>	-1.54 17.1	0.39 $\pm$ 2.16
Metrics Reloaded	-0.51 1.11	<b>0.07<math>\pm</math>0.20</b>	<b>-0.38 1.08</b>	<b>0.11<math>\pm</math>0.16</b>	-2.37 1.75	0.11 $\pm$ 0.20	-1.30 1.59	<b>0.09<math>\pm</math>0.19</b>
MONAI	-2.69 4.99	0.20 $\pm$ 0.70	-4.75 5.45	<b>0.11<math>\pm</math>0.86</b>	-37.5 14.5	<b>-0.01<math>\pm</math>2.78</b>	-1.54 17.1	0.39 $\pm$ 2.16
Plastimatch	-0.51 1.11	<b>0.07<math>\pm</math>0.20</b>	<b>-0.38 1.08</b>	<b>0.11<math>\pm</math>0.16</b>	-2.37 1.75	0.11 $\pm$ 0.20	-1.30 1.59	<b>0.09<math>\pm</math>0.19</b>
pymia	-1.36 1.06	-0.19 $\pm$ 0.34	-1.81 0.85	-0.53 $\pm$ 0.27	-2.63 2.87	-0.84 $\pm$ 0.48	-2.89 1.12	-0.35 $\pm$ 0.35
SimpleITK	-1.36 1.06	-0.19 $\pm$ 0.34	-1.81 0.85	-0.53 $\pm$ 0.27	-2.63 2.87	-0.84 $\pm$ 0.48	-2.89 1.12	-0.35 $\pm$ 0.35
$\Delta$ ASSD (mm)	min   max	Mean $\pm$ SD	min   max	Mean $\pm$ SD	min   max	Mean $\pm$ SD	min   max	Mean $\pm$ SD
Anima	-7.31 0.41	-1.06 $\pm$ 0.87	-5.63 -0.10	-1.07 $\pm$ 0.75	-13.5 1.96	-1.58 $\pm$ 1.23	-22.9 -0.22	-1.49 $\pm$ 2.92
Google DeepMind	-0.79  <b>-0.02</b>	-0.20 $\pm$ 0.09	-0.49  <b>-0.06</b>	-0.18 $\pm$ 0.06	<b>-0.50 -0.03</b>	-0.20 $\pm$ 0.07	<b>-0.48 -0.09</b>	-0.18 $\pm$ 0.06
Metrics Reloaded	<b>-0.42 1.58</b>	0.10 $\pm$ 0.20	<b>-0.37 1.72</b>	<b>0.12<math>\pm</math>0.17</b>	-4.55 2.89	<b>0.11<math>\pm</math>0.27</b>	-1.98 2.88	<b>0.11<math>\pm</math>0.30</b>
MONAI	<b>-0.42 1.58</b>	0.10 $\pm$ 0.20	<b>-0.37 1.72</b>	<b>0.12<math>\pm</math>0.17</b>	-4.55 2.89	<b>0.11<math>\pm</math>0.27</b>	-1.98 2.88	<b>0.11<math>\pm</math>0.30</b>
seg-metrics	-0.62 1.33	<b>-0.02<math>\pm</math>0.24</b>	-0.65 1.23	-0.13 $\pm$ 0.17	-4.09 1.81	-0.18 $\pm$ 0.23	-3.29 1.39	-0.13 $\pm$ 0.29
$\Delta$ NSD <sub><math>\tau=2</math> mm</sub> (%pt)	min   max	Mean $\pm$ SD	min   max	Mean $\pm$ SD	min   max	Mean $\pm$ SD	min   max	Mean $\pm$ SD
Google DeepMind	<b>-4.25 34.8</b>	4.03 $\pm$ 4.38	<b>-0.09 19.3</b>	3.46 $\pm$ 2.94	<b>-0.08 24.2</b>	4.07 $\pm$ 3.27	<b>-0.02 8.12</b>	1.34 $\pm$ 1.30
Metrics Reloaded	-16.1  <b>14.6</b>	<b>-0.30<math>\pm</math>3.13</b>	-15.2  <b>10.7</b>	<b>0.28<math>\pm</math>2.90</b>	-14.9  <b>12.8</b>	<b>0.48<math>\pm</math>3.20</b>	-6.41  <b>4.40</b>	<b>-0.49<math>\pm</math>1.55</b>
MONAI	-16.1  <b>14.6</b>	<b>-0.30<math>\pm</math>3.13</b>	-15.2  <b>10.7</b>	<b>0.28<math>\pm</math>2.90</b>	-14.9  <b>12.8</b>	<b>0.48<math>\pm</math>3.20</b>	-6.41  <b>4.40</b>	<b>-0.49<math>\pm</math>1.55</b>
pymia	<b>-4.25 34.8</b>	4.03 $\pm$ 4.38	<b>-0.09 19.3</b>	3.46 $\pm$ 2.94	<b>-0.08 24.2</b>	4.07 $\pm$ 3.27	<b>-0.02 8.12</b>	1.34 $\pm$ 1.30
$\Delta$ BioU <sub><math>\tau=2</math> mm</sub> (%pt)	min   max	Mean $\pm$ SD	min   max	Mean $\pm$ SD	min   max	Mean $\pm$ SD	min   max	Mean $\pm$ SD
Metrics Reloaded	<b>-19.6 38.3</b>	<b>6.32<math>\pm</math>9.01</b>	<b>-15.9 37.1</b>	<b>10.9<math>\pm</math>10.7</b>	<b>-9.66 35.0</b>	<b>10.4<math>\pm</math>10.4</b>	<b>-6.60 27.2</b>	<b>8.07<math>\pm</math>7.75</b>

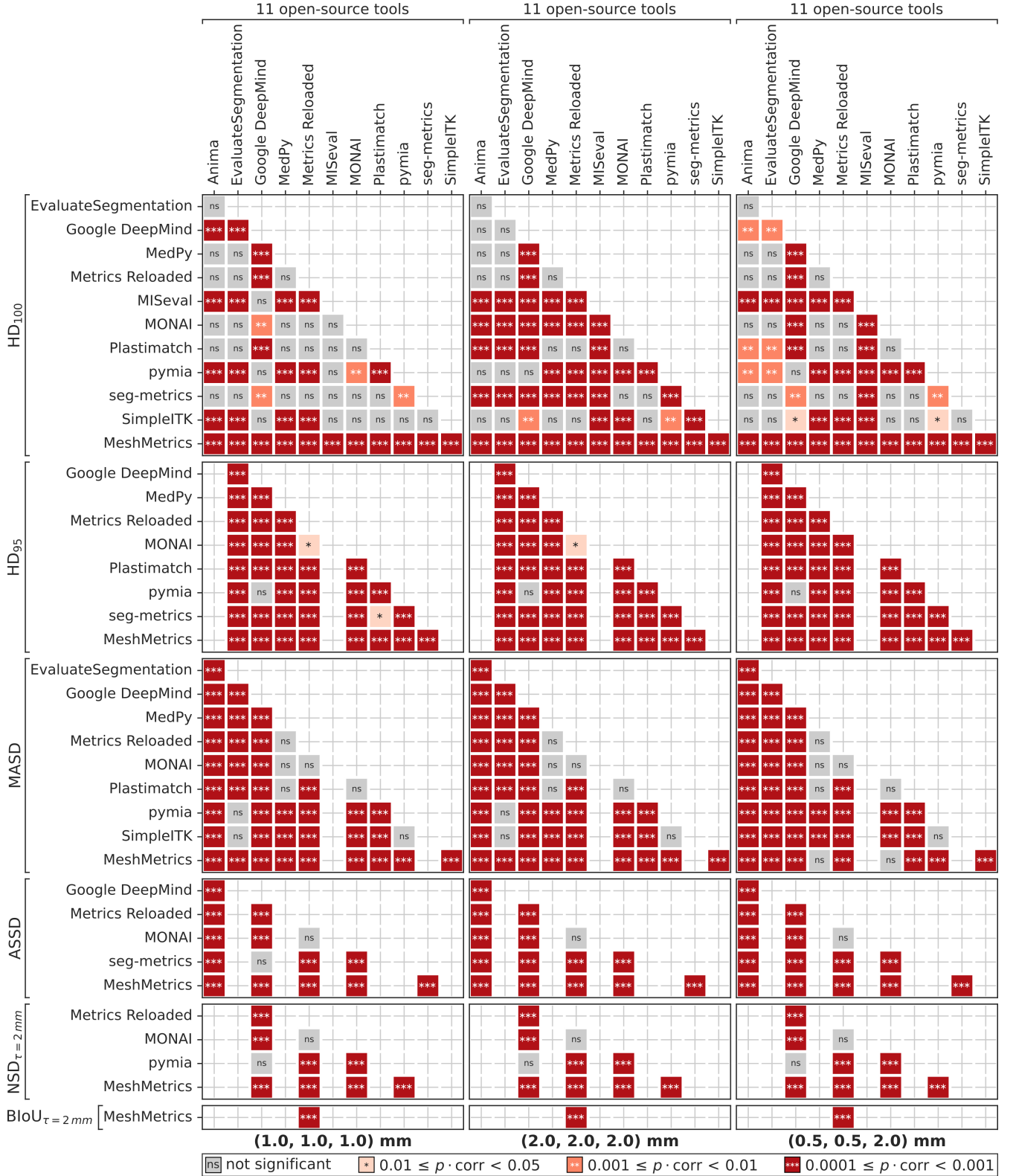


**Fig. A4.** Statistical testing of the open-source tools for distance-based metrics computation on 1,561 pairs of OAR segmentation masks, reported for two isotropic and one anisotropic voxel size. The value of  $\text{corr}$  is 1,188 and denotes the Bonferroni correction to adjust for the total number of comparisons and reduce the probability of Type I error.

**Table A3.** Edge case handling considering the input to open-source tools are two segmentation masks  $A$  and  $B$ . O1–O3 denote the output of each tool when  $A$  is an empty mask (O1),  $B$  is empty mask (O2) or both  $A$  and  $B$  are empty masks (O3), while S denotes whether the resulting metric score remains unchanged when the inputs are swapped. Besides all distance-based metrics, DSC is also included to provide a more comprehensive overview. <sup>‡</sup>Note that **Google DeepMind** does not originally support ASSD, but provides all necessary data for the user to simply compute it. We therefore omit the analysis of its edge case handling for this tool.

Open-source tool	DSC				HD				MASD				ASSD				NSD				BIoU							
	O1	O2	O3	S	O1	O2	O3	S	O1	O2	O3	S	O1	O2	O3	S	O1	O2	O3	S	O1	O2	O3	S				
<b>Anima</b> [11]	E*	0	E*	✓	E*	NaN	E*	✓	E*	NaN	E*	✓	E*	NaN	E*	✓					0	0	NaN <sup>W</sup>	✓				
<b>EvaluateSegmentation</b> [7]	E	E	E	✓	E	E	E	✗	E	E	E	✗																
<b>Google DeepMind</b> [12]	0	0	NaN	✓	∞	∞	∞	✓	NaN	NaN	NaN	✓				‡	0	0	NaN <sup>W</sup>	✓								
<b>MedPy</b> [13]	0	0	1	✓	E	E	E	✓	E	E	E	✗																
<b>Metrics Reloaded</b> [1]	0	0	1 <sup>W</sup>	✓	E	E	0	✓	E	E	0	✓					E	E	0	✓	0	0	NaN <sup>W</sup>	✓	0	0	NaN	✓
<b>MISeval</b> [8]	0	0	1	✓	$\mathbb{R}_{>0}$	$\mathbb{R}_{>0}$	0	✓																				
<b>MONAI</b> [14]	0	0	1	✓	NaN <sup>W</sup>	NaN <sup>W</sup>	NaN <sup>W</sup>	✓	∞ <sup>W</sup>	∞ <sup>W</sup>	NaN <sup>W</sup>	✗	∞ <sup>W</sup>	∞ <sup>W</sup>	NaN <sup>W</sup>	✓	0	0	NaN	✓								
<b>Plastimatch</b> [15]	0	0	0	✓	∞*	∞*	E	✓	∞*	∞*	E	✓																
<b>pymia</b> [16]	0	0	1	✓	∞ <sup>W</sup>	∞ <sup>W</sup>	∞	✓	∞ <sup>W</sup>	∞ <sup>W</sup>	∞	✓					0	0	−∞ <sup>W</sup>	✓								
<b>seg-metrics</b> [17]	0	0	0	✓	∞*	∞*	E	✓					∞*	∞*	E	✓												
<b>SimpleITK</b> [18]	0	0	∞	✓	E	E	E	✓	E	E	E	✓																
<b>MeshMetrics</b> (proposed)	0	0	NaN	✓	∞	∞	NaN	✓	∞	∞	NaN	✓	∞	∞	NaN	✓	0	0	NaN	✓	0	0	NaN	✓	0	0	NaN	✓

NaN: not a number, E: error message, E\*: empty string, no actual error message, W: additional warning message, ∞\*: a very large integer,  $\mathbb{R}_{>0}$ : a positive decimal number, ✓: yes, ✗: no

### Commentary:

There are considerable differences in how the open-source tools handle edge cases. For counting metrics like DSC, the approach is straightforward, as if only  $A$  or  $B$  is empty, DSC is set to zero. However, absolute distance-based metrics, such as HD, HD<sub>p</sub>, MASD and ASSD, present more challenges as they are bounded from below with zero. From a theoretical perspective, if  $A$  or  $B$  is empty, absolute metrics should return an infinite value. However, when both  $A$  and  $B$  are empty, the situation becomes more complex because the absence of the mask to compare to makes this scenario invalid for standard evaluation. The most appropriate response is that the tools return *not a number* (NaN) with a warning, leaving the user to substitute this score with the appropriate numeric value. On the other hand, relative distance-based metrics, such as NSD and BIoU, behave similarly to counting metrics. If  $A$  or  $B$  is empty, the result should be zero, while if both  $A$  and  $B$  are empty, the output could be 1, indicating a perfect match. However, to maintain consistency with absolute metrics, we suggest that the tools return NaN with a warning. While most open-source tools return either NaN, infinite values (∞) or very large integers (∞\*), or generate error messages (E) when edge case are encountered, we found some concerning irregularities. For example, random positive decimal values ( $\mathbb{R}_{>0}$ ) are returned by **MISeval** for HD when either  $A$  or  $B$  is empty and zero when both  $A$  and  $B$  are empty (this is problematic because it fails to distinguish between cases where only  $A$  or  $B$  is empty, and where both  $A$  and  $B$  are empty), negative infinity (−∞) is returned by **pymia** for NSD when both  $A$  and  $B$  are empty, while NaN is returned by **Google DeepMind** for MASD and **MONAI** for HD for all three edge cases. Although large positive integers can be considered acceptable outputs for command-line tools, such as **Plastimatch**, due to limitations in their value types (not supporting infinity), returning a positive decimal value or a zero distance is highly misleading and fundamentally incorrect. Special attention must be given to handling NaN and infinite values. Simply plotting these values using tools like *Seaborn boxplot* (Seaborn is a Python data visualization library) can lead to incorrect visualizations, as these values are ignored by default. If both  $A$  and  $B$  are empty, NaN suggests that detection and not segmentation is the primary task of investigation. Consequently, evaluation should be split into the detection and segmentation part, ensuring objectivity and facilitating comparison to other studies. In line with the recommendations from the *Metrics Reloaded* initiative, we suggest replacing infinite values with the largest distance in the image (e.g. the diagonal) or the maximum distance computed across all evaluations, and to document this decision in the corresponding study. On the other hand, the verification of swapped inputs did not reveal any new insights, as **EvaluateSegmentation** produces asymmetric results for HD<sub>95</sub> and MASD due to their non-deterministic calculation, while **MedPy** and **MONAI** exhibit asymmetry for MASD because both report the average *directed* distance.

### Conclusion:

While it is possible to handle edge cases by external conditioning (e.g. **if-then** statements), it is critical that the tools provide clear and informative outputs, especially for users who may be aware of their edge case handling behavior. Mishandling can lead to over-optimistic performance estimates, especially if edge cases are omitted from evaluation or are unjustifiably assigned the best possible metric score.

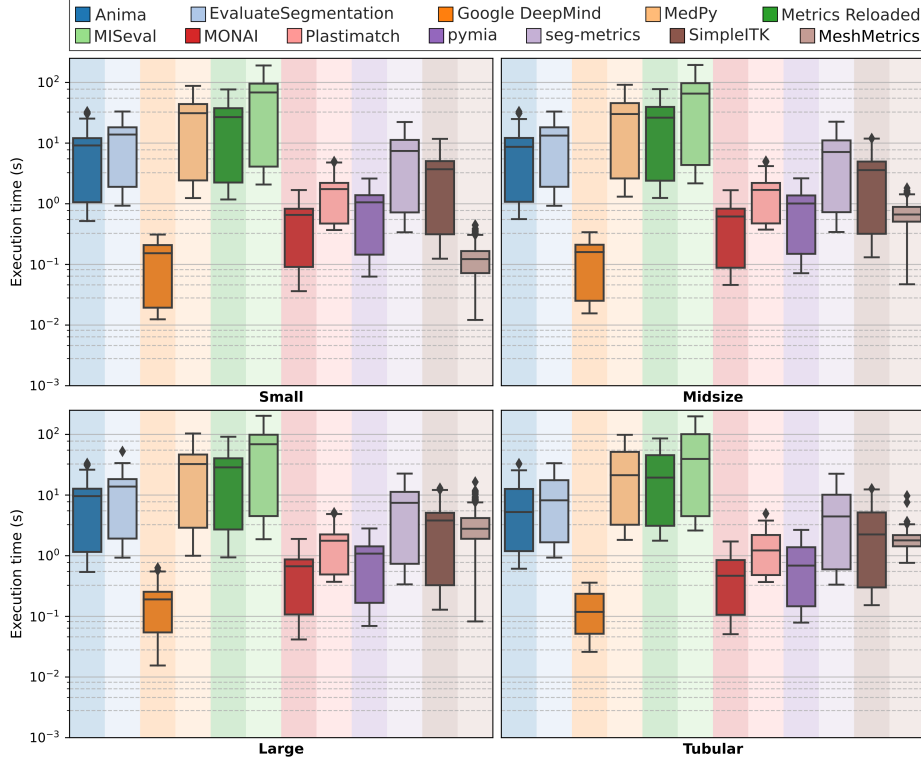


**Fig. A5.** Comparison of the HD computational efficiency across all 11 open-source tools and our reference implementation **MeshMetrics** on 1,561 pairs of OAR segmentation masks, reported for the voxel size of (1.0, 1.0, 1.0) mm and stratified by OAR categories, and shown in the form of box-plots. The analysis is focused solely on HD, because it is the only distance-based metric that is supported across all 11 open-source tools. When observing computational efficiency across different voxel sizes, the median execution time per case is the lowest for the small and midsize OARs, which is expected because of the lower number of query points needed for distance calculation. Across different open-source tools, **Google DeepMind** is identified as the most computationally efficient, followed by **MONAI** and **pymia**. In comparison, solid median execution times can be observed for **Plastimatch** and **SimpleITK**, while **Anima**, **EvaluateSegmentation**, **MedPy**, **Metrics Reloaded**, **MISEval** and **seg-metrics** are the least computationally efficient. The substantial differences in median execution times can be mostly attributed to the fact that **Google DeepMind**, **MONAI**, **Plastimatch** and **pymia** apply cropping to bounding box optimization, and therefore rank as most computationally efficient. On the other hand, our reference implementation **MeshMetrics** was designed to prioritize the accuracy of distance-based metrics computation, while the computational efficiency was not the primary focus of optimization. For example, after meshing we further subdivide each boundary element (in our case, each mesh triangle) into multiple sub-elements, which results in a larger number of query points for which the required distances have to be calculated, therefore considerably slowing down the overall computation. Nevertheless, it is interesting to observe that, in terms of the median execution time, **MeshMetrics** outperformed the majority of the open-source tools across all OAR categories. From the perspective of individual vs. simultaneous computation of multiple metrics, **Google DeepMind**, **Metrics Reloaded**, **Plastimatch**, **pymia**, **seg-metrics** and **SimpleITK** calculate the required distances only once and reuse them for simultaneous computation of multiple metrics, while **Anima**, **EvaluateSegmentation**, **MedPy**, **MISEval** and **MONAI** recalculate the required distances for each individual metric.



**Table A4.** The differences ( $\Delta$ ) in the distance-based metrics computed on 1,561 pairs of OAR segmentation masks, as obtained by meshing with the *marching cubes* and *surface nets* algorithms against the *discrete marching cubes* algorithm that is used by our reference implementation *MeshMetrics* (cf. Fig. A2), reported for two isotropic and one anisotropic voxel size as the range min|max and mean  $\pm$  standard deviation (SD).

Open-source tool	Voxel size					
	(1.0, 1.0, 1.0) mm		(2.0, 2.0, 2.0) mm		(0.5, 0.5, 2.0) mm	
<b><math>\Delta</math> HD (mm)</b>	min max	Mean $\pm$ SD	min max	Mean $\pm$ SD	min max	Mean $\pm$ SD
Marching cubes	<b>-0.00 0.08</b>	<b>0.00<math>\pm</math>0.00</b>	<b>-0.37 0.54</b>	<b>0.00<math>\pm</math>0.02</b>	<b>-0.10 0.15</b>	<b>0.00<math>\pm</math>0.01</b>
Surface nets	-1.26 1.08	-0.15 $\pm$ 0.26	-2.20 3.28	-0.22 $\pm$ 0.45	-0.92 0.83	-0.09 $\pm$ 0.19
<b><math>\Delta</math> HD<sub>p</sub> (mm)</b>	min max	Mean $\pm$ SD	min max	Mean $\pm$ SD	min max	Mean $\pm$ SD
Marching cubes	<b>-0.15 0.10</b>	<b>-0.00<math>\pm</math>0.01</b>	<b>-1.51 0.34</b>	<b>-0.01<math>\pm</math>0.07</b>	<b>-0.55 0.07</b>	<b>-0.00<math>\pm</math>0.02</b>
Surface nets	-1.32 1.15	-0.17 $\pm$ 0.22	-2.64 2.75	-0.18 $\pm$ 0.37	-1.26 0.54	-0.17 $\pm$ 0.19
<b><math>\Delta</math> MASD (mm)</b>	min max	Mean $\pm$ SD	min max	Mean $\pm$ SD	min max	Mean $\pm$ SD
Marching cubes	<b>-0.03 0.02</b>	<b>-0.00<math>\pm</math>0.00</b>	<b>-0.11 0.10</b>	<b>-0.00<math>\pm</math>0.01</b>	<b>-0.02 0.02</b>	<b>0.00<math>\pm</math>0.00</b>
Surface nets	-0.82 0.20	-0.14 $\pm$ 0.07	-1.47 0.56	-0.16 $\pm$ 0.12	-0.61 0.07	-0.10 $\pm$ 0.06
<b><math>\Delta</math> ASSD (mm)</b>	min max	Mean $\pm$ SD	min max	Mean $\pm$ SD	min max	Mean $\pm$ SD
Marching cubes	<b>-0.03 0.04</b>	<b>-0.00<math>\pm</math>0.00</b>	<b>-0.20 0.21</b>	<b>-0.00<math>\pm</math>0.01</b>	<b>-0.03 0.03</b>	<b>0.00<math>\pm</math>0.00</b>
Surface nets	-1.53 0.22	-0.14 $\pm$ 0.09	-2.15 0.88	-0.17 $\pm$ 0.15	-0.84 0.15	-0.11 $\pm$ 0.07
<b><math>\Delta</math> NSD <math>\tau=2</math> mm (%pt)</b>	min max	Mean $\pm$ SD	min max	Mean $\pm$ SD	min max	Mean $\pm$ SD
Marching cubes	<b>-0.49 0.49</b>	<b>0.00<math>\pm</math>0.04</b>	<b>-3.28 2.02</b>	<b>0.00<math>\pm</math>0.21</b>	<b>-0.44 0.51</b>	<b>0.00<math>\pm</math>0.04</b>
Surface nets	-2.79 12.7	2.29 $\pm$ 1.95	-7.55 25.6	2.80 $\pm$ 2.74	-2.67 8.53	1.65 $\pm$ 1.45
<b><math>\Delta</math> BIoU <math>\tau=2</math> mm (%pt)</b>	min max	Mean $\pm$ SD	min max	Mean $\pm$ SD	min max	Mean $\pm$ SD
Marching cubes	<b>-14.6 54.8</b>	4.22 $\pm$ 4.63	<b>-11.9 41.8</b>	5.07 $\pm$ 5.01	<b>-17.6 66.2</b>	3.97 $\pm$ 5.25
Surface nets	-32.2 14.1	<b>1.09<math>\pm</math>4.56</b>	-32.6 23.7	<b>1.50<math>\pm</math>5.52</b>	-45.0 10.3	<b>-0.10<math>\pm</math>4.46</b>